Journal Pre-proof

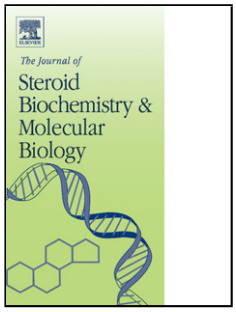

Synthesis and anti–tumour, immunomodulating activity of diosgenin and tigogenin conjugates

O. Michalak, P. Krzeczyński, M. Cieślak, P. Cmoch, M. Cybulski, K. Królewska-Golińska, J. Kaźmierczak-Barańska, B. Trzaskowski, K. Ostrowska

PII: S0960-0760(19)30352-8

DOI: https://doi.org/10.1016/j.jsbmb.2019.105573

Reference: SBMB 105573

To appear in: *Journal of Steroid Biochemistry and Molecular Biology*

Received Date: 13 June 2019

Revised Date: 20 December 2019

Accepted Date: 23 December 2019

Please cite this article as: Michalak O, Krzeczyński P, Cieślak M, Cmoch P, Cybulski M, Królewska-Golińska K, Kaźmierczak-Barańska J, Trzaskowski B, Ostrowska K, Synthesis and anti–tumour, immunomodulating activity of diosgenin and tigogenin conjugates, *Journal of Steroid Biochemistry and Molecular Biology* (2020), doi: https://doi.org/10.1016/j.jsbmb.2019.105573

Synthesis and anti–tumour, immunomodulating activity of diosgenin and tigogenin conjugates

O. Michalak[a]*, P. Krzeczyński[a], M. Cieślak[b], P. Cmoch[c], M. Cybulski[a], K. Królewska–Golińska[b], J. Kaźmierczak–Barańska[b], B. Trzaskowski[d], K. Ostrowska[e]

[a] *Łukasiewicz Research Network–Pharmaceutical Research Institute, 8 Rydygiera Str., 01–793 Warsaw, Poland*

[b] *Department of Bioorganic Chemistry, Centre of Molecular and Macromolecular Studies, Polish Academy of Sciences, 112 Sienkiewicza Str., 90–363 Łódź, Poland*

[c] *Institute of Organic Chemistry, Polish Academy of Sciences, 44/52 Kasprzaka Str., 01–224, Warsaw, Poland*

[d] *Chemical and Biological Systems Simulation Lab, Center of New Technologies, University of Warsaw, 2C Banacha Str., 02–097 Warsaw, Poland*

[e] *Department of Organic Chemistry, Faculty of Pharmacy, Medical University of Warsaw, 1 Banacha Str., 02–097 Warsaw, Poland*

*****Correspondence: Łukasiewicz Research Network–Pharmaceutical Research Institute, 8 Rydygiera Str., 01–793 Warsaw, Poland; o.michalak@ifarm.eu; Tel. +48 22 456 3925

Graphical abstract

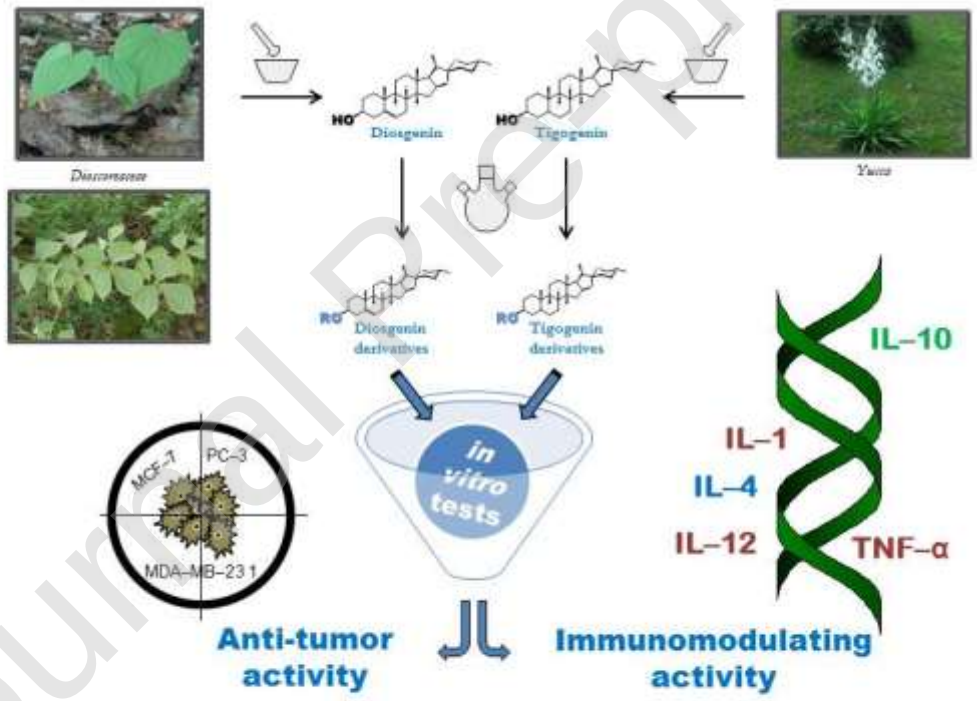

Highlights

- A set of diosgenin and tigogenin derivatives substituted with various amino acids, dipeptides or levulinic and 3,4–dihydroxycinnamic acid were synthesized
- Analogue **2c** (*L*–serine in position 3 of tigogenin) showed the highest activity against the breast
- cancer cell line (MCF–7) and its affinity profile to the active site of the estrogen receptor (ER) was confirmed by molecular docking
- A diosgenin derivative with caffeic acid **16a** and the analogue of tigogenin with glutamic acid **4c**
- exhibited preferred immunomodulatory effects
- A strong binding interaction of compounds **4c** and **16a** (Ki=0.23 pM and Ki=1.14 pM) with the active site of the glucocorticoid receptor (GR) was estimated using molecular docking

Abstract:

A series of novel diosgenin (DSG) and tigogenin (TGG) derivatives with diosgenin or tigogenin steroid aglycons linked to levulinic and 3,4–dihydroxycinnamic acids, dipeptides and various amino acids by an ester bond at the C3–oxygen atom of the steroid skeleton has been synthesized. Diosgenyl esters have been prepared by an esterification reaction (DCC/DMAP) of diosgenin with the corresponding acids.

All analogues have been evaluated *in vitro* for their antiproliferative profile against cancer cell lines (MCF–7, MDA–MB–231, PC–3) and human umbilical vein endothelial cells (HUVEC). Analogue **2c** (*L*–serine derivative of TGG), the best representative of the series showed IC_{50} of 1.5 μM (MCF–7), and induced apoptosis in MCF–7 by activating caspase–3/7.

The immunomodulatory properties of six synthesized analogues have been determined by examining their effects on the expression of cytokine genes essential for the functioning of the human immune system (IL–1, IL–4, IL–10, IL–12 and TNF–α). Biological evaluation has revealed that new compounds **4c** and **16a** do not induce the expression of pro–inflammatory cytokines in THP–1 cells after the lipopolysaccharide (LPS) stimulation. They also stimulate the expression of anti–inflammatory IL–10 that acts stronger than diosgenin itself.

An in silico ADME (properties, absorption, distribution, metabolism, excretion) study was also performed to predict the pharmacokinetic profile of the synthesized compounds. To shed light on the molecular interactions between the synthesized compounds and the glucocorticoid receptor and the estrogen receptor, **2c**, **4c** and **16a** compounds were docked into the active binding sites of these receptors.

The *in silico* and *in vitro* data suggested that this new group of compounds might be considered as a promising scaffold for further modification of more potent and selective anticancer and immunomodulatory agents.

Keywords

Diosgenin, Tigogenin, Inflammation, Cancer, Anti–tumor, Docking

1. Introduction

Due to their interesting biological properties, natural compounds have recently attracted much attention of both academics and pharmaceutical industry. This also applies to steroidal saponins which are not only basic precursors for the synthesis of the sex hormones and corticosteroids in the pharmaceutical industry, but also display various types of pharmacological activity, such as antibacterial, anti–inflammatory, anticancer and hypocholesterolemic [1].They are therefore expected to become key building blocks of new drugs with different signal transduction properties.

Diosgenin and tigogenin belong to the group of steroidal saponins. Diosgenin is present mainly in the *Dioscoreaceae* plant family, but also in some species of *Solanaceae* and *Fabaceae* families in combination with various sugars in the glycosides form, such as dioscin and gracilin. Tigogenin is isolated from Yucca (*Agavaceae*) [1], but its triglycoside is isolated from the genus *Hosta* and *Tribulus*plants [2] (Fig.1).

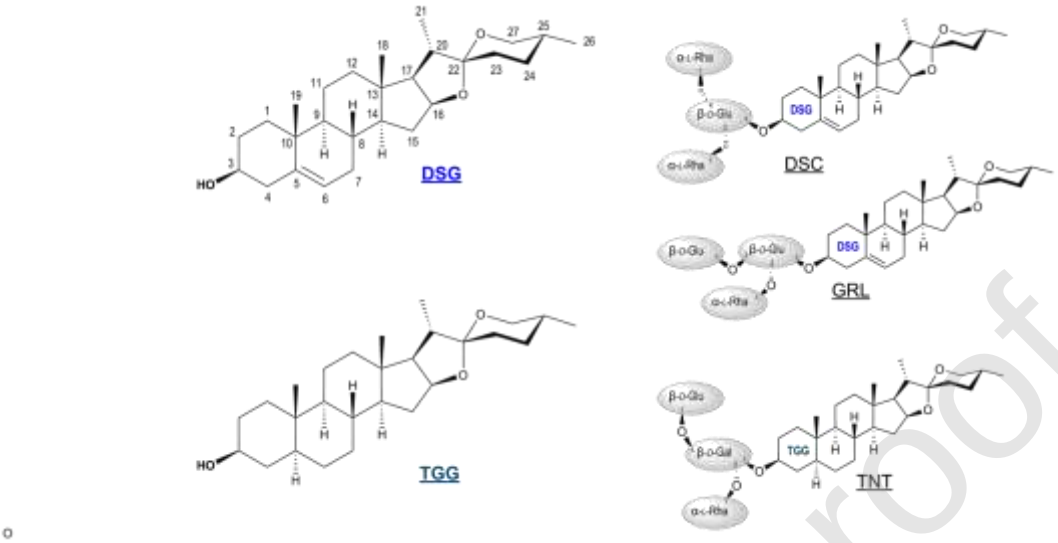

Fig.1. Diosgenin (DSG), tigogenin (TGG) and their natural glycosides:
dioscin (DSC), gracilin (GRL) and tigogenin natural triglicoside (TNT)

Diosgenin and diosgenyl glycosides display, among others, antiviral, anti–inflammatory, antidiabetic and anticancer activity [3], while tigogenin triglycoside has been widely used in China as a traditional medicine against various diseases [4]. *In vitro* assays have revealed that tigogenin has a very weak anti–proliferative activity [5], but tigogenin triglycoside and its three derivatives bearing different carbohydrate moieties exhibit a potent cytostatic activity against human promyelocytic leukemia HL–60 cells and human epithelial cervical cancer cells [2]. Guo–Long L. et al. have synthesized a series of tigogenin neoglycosides and their *in vitro* antitumor activity against five human cancer cell lines has been evaluated. Some tigogenin neoglycosides have displayed enhanced antitumor activity against one or more human cancer cell lines [6].

Diosgenin's anticancer potential has been extensively studied both *in vitro* and *in vivo* [7]. The *in vitro* studies have been performed on various human cancer cell lines to confirm the influence of diosgenin on various molecular targets critical for carcinogenesis. It has been shown that diosgenin inhibited the proliferation of HT–29 human colon cancer cells and induced apoptosis partly by modulating the expression of bcl–2 and caspase–3 *in vitro* [8]. In the HCT–116 human colon cancer cells diosgenin has modulated the expression of 3–hydroxy–3–methylglutaryl–CoA reductase (HMG–CoA), the enzyme that inhibits the biosynthesis of cholesterol [9]. Diosgenin has been reported to induce selective apoptosis in AU565 human breast adenocarcinoma cells through PARP cleavage [10]. It has been demonstrated that diosgenin displays a significant anticancer activity against both the estrogen receptor positive (ER+) and estrogen receptor negative (ER−) breast cancer cell lines by inhibiting prosurvival signaling pathways Akt, Raf/MEK, NF–κB and inducing apoptosis [11]. The compound also inhibits the proliferation of PC–3 human prostate cancer cells due to the reduction of the activity as well as the mRNA expression of MMP–2 (matrix metalloproteinase) and MMP–9 [12]. It has been shown that diosgenin suppresses the proliferation of hepatocellular carcinoma (HCC) at the G1 phase of the cell cycle and inhibits both constitutive and inducible activation of STAT3 with no effect on STAT5 [13]. Diosgenin also causes the G2/M cell cycle arrest and apoptosis in human leukemia K562 cells [14].

In addition, it has been shown that both diosgenin and tigogenin inhibit growth and induce apoptosis of synovial cells *in vitro* (human cells of the synovial membrane) which play a significant role in rheumatoid arthritis [15]. It has also been reported that diosgenin exhibits an anti–inflammatory activity by downregulating the TNF–α–induced expression of ICAM–1 via the inhibition of NF–κB p65 activation [16]. Both specific and non–specific cellular immune responses might be supported by diosgenin action which indirectly exerts an anti–tumour effect by activating the immune system [17].

M. Singh et al. have synthesized several analogues of diosgenin by modifying the spiroketal ring. They have demonstrated that diosgenin analogues inhibit the production of pro–inflammatory cytokines (TNF–α, IL–6 and IL–1β) both under *in vitro* and *in vivo* conditions [18].

Romero–Hernández et al. have proved that newly obtained thioxo and selenoxo diosgenin derivatives behave as strong antiproliferative agents against human tumor cells, with a higher potency than that of diosgenin itself [19]. Kvasnica et al. [20] have studied the anticancer activity of the platinum (II) compounds conjugated with *L*–histidine and *L*–methionine esters with various steroids, including diosgenin. Some compounds have displayed a significant cytotoxic activity towards acute lymphoblastic leukaemia CEM cell lines with the IC_{50} values in the 14–25 μM range.

B. Huang et al. have synthesized several diosgenyl esters of primary amino acids and their *N*–salicylamides [21]. The compounds have been MTT–tested to evaluate their cytotoxic activity against the cell lines of human breast carcinoma MDA–MB–231, mouse colon cancer C26 and human hepatocellular cancer Hep G2. The diosgenin analogue substituted with the 6–aminohexanoic acid moiety at position C–3 of the steroid core structure (aminocaproic acid analogue) proves to be more effective than aspirin or diosgenin alone against all three tested cancer cell lines. The IC_{50} values range from 4.7 μM against the C26 cells to 14.6 μM against HepG2 cells. Moreover, in the anti–inflammatory activity test several salicylate conjugates have significantly inhibited ear swelling caused by xylene, displaying comparable or stronger anti–inflammatory activity than that of diosgenin and aspirin, whereas among other esters only the aminocaproic acid analog has exhibited similar characteristics to that of the reference compounds.

While studying the influence of the structure on the anticancer activity and anticoagulant properties, the same authors [22] have obtained three series of diosgenyl esters with different aglycone skeleton structures. Compounds with the side chains including 4–8 carbon atoms displayed a much stronger inhibitory activity towards cancer cell lines (C26 (colon), B16 (melanoma), HepG2 (liver), A549 (lung), MDA–MB–231 (breast)) than diosgenin itself or its analogues with shorter or longer carbon chains. Among the studied compounds, the one with the 6–aminocaproic moiety including six carbon atoms was more active than other analogues, especially against C26 cell lines (IC_{50} 5.5 μM).

R. Ur Masood et al. have synthesized novel triazoles of diosgenin and have evaluated their anti–proliferative activity against several human cancer cell lines: breast (HBL–100), lung (A–549), colon (HT–29 and HCT–116). Five analogues have been identified as potent antiproliferative agents against all the tested cancer cells [23].

Several novel analogues of diosgenin at C7 position have been prepared by Hamid et al. Six of the analogues exhibit anticancer activity against a panel of human cancer cell lines with IC_{50} ranging from 12 to 35 μM. Additionally, these analogues inhibit lipopolysaccharideinduced pro–inflammatory cytokines (TNF–α and IL–6) [24].

The above mentioned studies demonstrate that diosgenin analogues substituted at position C–3 of the steroid core structure possess a significant antitumor activity. Their immunomodulating profiles are poorly studied, which we have considered worth investigating. Thus, it was assumed that the evaluation of new substituents at position C3 may be of interest from the point of view of optimizing diosgenin analogues as potential therapeutic agents (anticancer or immunomodulatory). For *in vitro* biological evaluation we have selected the following cancer cell lines: PC3, MCF–7, MDA–MB–231

[25] due to the fact that prostate cancer is the second most frequently diagnosed cancer in men (15% of all male cancers) and breast cancer among women (25% of all female cancers).

This work reports the synthesis of diosgenin derivatives with new structural fragments at position C3, such as: levulinic and 3,4–dihydroxycinnamic acids, dipeptides and various amino acids. Steroid aglycons have been connected to new substituents by an ester bond at the C3–oxygen atom of their skeleton. The hydrogenation of the double bond at the C5–C6 position of new diosgenin amino acid derivatives has led to new tigogenin analogues. All compounds have been evaluated for their antiproliferative activity *in vitro* against HUVEC and selected cancer cell lines. Particular derivatives have been examined for their influence on the inflammatory response.

2. Materials and methods

2.1. Abbreviations

AcOEt — ethyl acetate; Boc — tert–butyloxycarbonyl group; DCC— *N*,*N′*–dicyclo-hexylocarbodiimide; DCU — Dicyclohexylurea; DCM — dichloromethane; DIPEA — *N*,*N*–diisopropylethylamine; DMAP — 4–dimethylaminopyridine; HCl — hydrochloric acid; HOBt — *N*–hydroxybenzotriazole monohydrate; MS — mass spectrometry; NMR — nuclear magnetic resonance; TBTU — *O*–(1*H*–benzotriazol–1–yl)–1,1,3,3–tetramethyluronium tetrafluoroborate; TEA — triethylamine; THF — tetrahydrofuran; TMS — trimethylsilyl; caff — caffeic acid; LPS — lipopolysaccharide; PC3 — prostate human cancer cell lines; MCF–7, MDA–MB–231— breast cancer cell lines; HCC— hepatocellular carcinoma; C26— colon cancer cell lines; HepG2— human liver cancer cell line; K562—human leukemia cell line; B16 — melanoma murine cell lines; HBL–100 — breast cancer cell lines; A–549 — lung cancer cell lines; HT–29 and HCT–116 — colon cancer cell lines; s, d, t, m_{ov} — singlet, doublet, triplet and overlapping multiplet/s in NMR spectra.

2.2. General procedures

Diosgenin was procured from KOCH–LIGHT LABORATORIES, UK. Other materials, solvents and reagents were of commercial origin and used without additional operations. Reactions were monitored on the silica gel TLC plates 60 F_{254} (Merck, Darmstadt, Germany). The visualization was performed by UV light (254 and/or 365nm) then with CeMo stain and subsequent charring [26]. Melting points were determined by the Melting Point System (Mettler Toledo MP70). Solvents were evaporated under reduced pressure at 40°C on the Büchi Rotavapor. Flash column chromatography was performed on silica gels (200–300 mesh).

The ^{1}H NMR and ^{13}C NMR spectra were recorded in $CDCl_3$ (protected diosgenin derivatives **2**–**18**, **16a**, **2b** and **4b**) and CD_3OD (**2a**–**3a**, **5a**–**14**, **2c** and **4c**) solutions with the Varian–NMR–vnmrs600 spectrometer (at 298 K) equipped with a 600 MHz PFG Auto XID (^{1}H/^{15}N–^{31}P 5 mm) indirect probehead. Standard experimental conditions and standard Varian programs (ChemPack 4.1) were used. To identify the structures of all isolated products correctly, a careful analysis of the results of 1D and 2D NMR experiments was performed. The 1D and 2D measurements covered: ^{1}H selective NOESY, 2D: COSY, NOESY, ^{1}H–^{13}C gradient selected (g–HSQC) and (g–HMBC) optimized for ^{1}J(C–H) = 150 Hz and ^{n}J(C–H) = 8 Hz, respectively. The ^{1}H and ^{13}C NMR chemical shifts are given relative to the TMS signal at δ = 0.0 ppm. The concentration of the solutions used for the measurements was about 10–20 mg of the compounds in 0.6 cm^3 of the solvent.

The mass spectra were recorded on the MaldiSYNAPT G2–S HDMS (Waters) Spectrometer via electrospray ionization (ESI–MS). High–resolution mass spectrometry (HRMS) measurements were performed using the Synapt G2-Si mass spectrometer (Waters) equipped with an ESI source and a quadrupole–Time–of–flight mass analyzer. The results of the measurements were processed using the MassLynx 4.1 software (Waters).

2.2. Chemical synthesis

The studied compounds were synthesized starting from diosgenin (**1**), as shown below (Scheme 1).

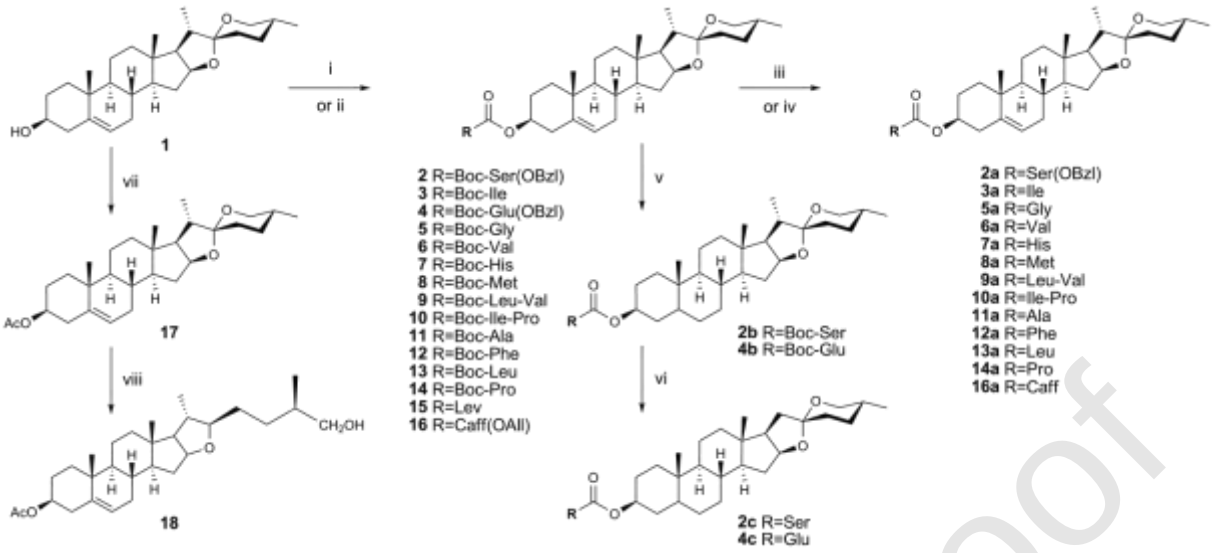

Scheme 1. i) DCC, DMAP, DCM, r.t; ii) TBTU, HOBt, DIPEA, DCM, r.t.; **2**–**16** yield 60–98%; iii) HCl/AcOEt, r.t.; **2a**–**14a** yield 63–93%; iv) 1,3–dimethylbarbituric acid, Ph_3P, $Pd(OAc)_2$, EtOH, 75°C; **16a** yield 98%; v) H_2, Pd/C, AcOEt, r.t.; **2a**, **4b** yields 79%, 94%; vi) HCl/AcOEt, r.t; **2c**, **4c** yields 65%, 70%; vii) Ac_2O, DMAP, TEA, DCM, r.t.; yield 83%; viii) $NaBH_3CN$, Ac_2O, r.t., yield 98%.

*2.2.1.General procedure for the synthesis of compounds **2**–**16***

*2.2.1.1. Synthesis of analogue **2** — (25R)–spirost–5–en–3β–yl N–(t–butoxycarbonyl)–O–benzyl–L–serinate*

DMAP (40 mg, 0.327 mmol) and DCC (280 mg, 1.357 mmol) were added to the solution of Boc–*L*–Ser(Bzl)–OH (400 mg, 1.354 mmol) in anhydrous CH_2Cl_2 (10 mL) and the mixture was stirred for 10 min at room temperature. Then diosgenin (406 mg, 0.979 mmol) was added and the reaction mixture was stirred at room temperature for 24 h (TLC control). After the reaction had been completed, the DCU precipitate was filtered off. The filtrate was washed successively with the $NaHCO_3$ aq. solution and NaCl aq. solution. The extract was dried over anhydrous $MgSO_4$, filtered and evaporated to dryness. The crude product was purified through a silica gel column eluted with ethyl acetate–hexane. Yield 93%, white solid, m.p. 161.6°C; $[M+H]^+$ calcd for $C_{42}H_{62}NO_7$: 692.4526, found: 692.4531, $[M+Na]^+$ calcd for $C_{42}H_{61}NO_7Na$: 714.4346, found: 714.4352.

^{1}H NMR ($CDCl_3$) δ [ppm]: *L*–serine part: 7.33 and 7.28 (5H, 2×m, phenyl), 5.39 (d, *J* = 8.8 Hz, NH), 4.56 and 4.47 (2H, 2×*J* = 12.2 Hz, both H4' protons), 4.39 (1H, m, H2'), 3.87 and 3.68 (2H, 2×dd, J = 2.9 and 9.2 Hz/3.0 and 9.2 Hz, both H3' protons), 1.45 (9H, s, 3×CH_3 of *t*–Bu), Diosgenin (**DSG**) part: 5.36 (1H, m, H5), 4.67 (1H, m, H3), 4.41 (1H, m, H16), 3.47 (1H, m, one of H27 protons), 3.38 (1H, t, *J* = 11.0 Hz, one of H27 protons), 2.27 (2H, m, both H4), 2.01 and 1.56 (2H, m_{ov}, both H7), 1.99 and 1.29 (2H, m_{ov}, both H15), 1.88 and 1.58 (2H, m_{ov}, both H2), 1.86 and 1.13 (2H, m_{ov}, both H1), 1.87 (1H, m_{ov}, H20), 1.78 (1H, m_{ov}, H17), 1.74 and 1.19 (2H, m_{ov}, both H12), 1.69 and 1.59 (2H, m_{ov}, both H23), 1.63 (1H, m_{ov}, H8), 1.62 and 1.45 (2H, m_{ov}, both H24), 1.62 (1H, m_{ov}, H25), 1.51 and 1.46 (2H, m_{ov}, both H11), 1.12 (1H, m_{ov}, H14), 1.02 (3H, s, CH_3–19), 0.98 (1H, m, H9), 0.97 (3H, d, *J* = 7.0 Hz, CH_3–21), 0.79 (6H, s and d (both overlapping), 2×CH_3 group: CH_3–18 and CH_3–26),

^{13}C NMR δ [ppm]: *L*–serine part: 170.0 (C1'), 155.5 (NH<u>C</u>O), [137.6, 128.4, 127.8, 127.6 – phenyl ring], 79.8 (O<u>C</u>(CH_3)$_3$), 73.3 (C4'), 70.2 (C3'), 54.2 (C2'), 28.3 (OC(<u>C</u>H_3)$_3$),

DSG part: 139.5 (C5), 122.5 (C6), 109.3 (C22), 80.9 (C16), 75.2 (C3), 66.9 (C27), 62.1 (C17), 56.4 (C14), 49.9 (C9), 41.6 (C20), 40.3 (C13), 39.7 (C12), 37.9 (C4), 36.9 (C1), 36.7 (C10), 32.1 (C7), 31.9 (C15), 31.4 (2C, C8 and C23), 30.3 (C25), 28.8 (C24), 27.7 (C2), 20.8 (C11), 19.3 (C19), 17.1 (C26), 16.3 (C18), 14.5 (C21).

Analogue **3** — (25*R*)–spirost–5–en–3β–yl *N*–(*t*–butoxycarbonyl)–*L*–isoleucinate:

yield 98%, white solid, m.p. 181.7°C; $[M+H]^+$ calcd for $C_{38}H_{62}NO_6$: 628.4577, found: 628.4582; $[M+Na]^+$ calcd for $C_{38}H_{61}NO_6Na$: 650.4397, found: 650.4406.

^{1}H NMR δ [ppm]: *L*–isoleucine part: 5.04 (1H, d, *J* = 8.7 Hz, NH), 4.22 (1H, dd, *J* = 4.5, 8.7 Hz, H2'), 1.85 (1H, m_{ov}, H3'), 1.44 (10H, s, one of H4' protons and nine protons of *t*–Bu), 1.18 (1H, m_{ov}, one of H4' protons), 0.93 (6H, 2×d, *J* = 7.0 Hz, CH_3 at C3' and CH_3–5') + **DSG** part,

^{13}C NMR δ [ppm]: *L*–isoleucine part: 171.6 (C1'), 155.5 (NH<u>C</u>O), 79.6 (O<u>C</u>$(CH_3)_3$), 57.9 (C2'), 38.2 (C3'), 28.3 (OC($\underline{C}H_3)_3$), 25.1 (C4'), 15.5 (CH_3 at C3') and 11.7 (CH_3–5') + **DSG** part.

Analogue **4** — (25*R*)–spirost–5–en–3β–yl *N*–(*t*–butoxycarbonyl)–5–benzyl–*L*–glutamate:

yield 94%, white solid, m.p. 154.7°C; $[M+H]^+$ calcd for $C_{44}H_{64}NO_8$: 734.4632, found: 734.4633, $[M+Na]^+$ calcd for $C_{44}H_{63}NO_8Na$: 756.4451, found: 756.4454.

^{1}H NMR δ [ppm]: *L*–glutamic acid part: 7.38–7.31 (5H, m, phenyl), 5.12 (2H, s, H6'), 5.09 (1H, d, *J* = 8.6 Hz, NH), 4.29 (1H, m, H2'), 2.47 and 2.44 (2H, 2 overlapping multiplets, both H4'), 2.20 and 1.95 (2H, m and part of overlapping multiplets, both H3'), 1.44 (9H, s, protons of *t*–Bu) + **DSG** part,

^{13}C NMR δ [ppm]: *L*–glutamic acid part: 172.6 (C5'), 171.6 (C1'), 155.4 (NH<u>C</u>O), [135.8, 128.6, 128.3 128.2 – phenyl ring], 79.9 (O<u>C</u>$(CH_3)_3$), 66.5 (C6'), 53.0 (C2'), 30.3 (C4'), 28.3 (OC($\underline{C}H_3)_3$), 27.9 (C3') + **DSG** part.

Analogue **5** — (25*R*)–spirost–5–en–3β–yl *N*–(*t*–butoxycarbonyl)–glycinate:

yield 90%, white solid, m.p. 137.4°C; $[M+H]^+$ calcd for $C_{34}H_{54}NO_6$: 572.3951, found: 572.3961, $[M+Na]^+$ calcd for $C_{34}H_{53}NO_6Na$: 594.3771, found: 594.3784.

^{1}H NMR δ [ppm]: glycine: 5.00 (1H, br), 3.88 (2H, m), 1.45 (9H, *t*–Bu) + **DSG** part,

^{13}C NMR δ [ppm]: glycine: 169.7 (C1'), 155.7 (NH<u>C</u>O), 79.9 (O<u>C</u>$(CH_3)_3$), 42.6 (C2'), 28.3 (OC($\underline{C}H_3)_3$) + **DSG** part.

Analogue **6** — (25*R*)–spirost–5–en–3β–yl *N*–(*t*–butoxycarbonyl)–*L*–valinate:

yield 98%, white solid, m.p. 137.5°C; $[M+H]^+$ calcd for $C_{37}H_{60}NO_6$: 614.4421, found: 614.4420, $[M+Na]^+$ calcd for $C_{37}H_{59}NO_6Na$: 636.4240, found: 636.4240.

^{1}H NMR δ [ppm]: *L*–valine: 5.02 (1H, d, *J* = 8.8 Hz), 4.17 (1H, dd, *J* = 4.6, 8.8 Hz, H2'), 1.45 (9H, s, *t*–Bu), 2.12 (1H, m_{ov}, H3'), 0.95 and 0.88 (both CH_3 groups at C3') + **DSG** part,

^{13}C NMR δ [ppm]: *L*–valine part: 171.7 (C1'), 155.7 (NH<u>C</u>O), 79.9 (O<u>C</u>$(CH_3)_3$), 58.5 (C2'), 31.4 (C3'), 28.3 (OC($\underline{C}H_3)_3$), 18.9 and 17.5 (both CH_3 groups at C3') + **DSG** part.

Analogue **7** — (25*R*)–spirost–5–en–3β–yl N^{α},N^{τ}–bis(*t*–butoxycarbonyl)–*L*–histidinate:

yield 94%, white solid, m.p. 163.2°C; $[M+H]^+$ calcd for $C_{43}H_{66}N_3O_8$: 752.4850, found: 752.4860.

^{1}H NMR δ [ppm]: *L*–histidine part: 8.00 (1H, s, H6'), 7.14 (1H, s, H8'), 5.67 (1H, d, *J* = 8.4 Hz, NH), 4.51 (1H, m, H2'), 3.03 (2H, m, H3'), 1.60 (9H, s, *t*–Bu at N7 of imidazole), 1.44 (9H, s, *t*–Bu at NH at C2') + **DSG** part,

^{13}C NMR δ [ppm]: 171.1 (C1'), 155.5 (NH<u>C</u>O), 146.8 (NH<u>C</u>O – imidazole), 138.7 (C4' – imidazole), 136.8 (C6' – imidazole), 114.6 (C8' – imidazole), 85.5 (O<u>C</u>$(CH_3)_3$ – imidazole), 79.9 (O<u>C</u>$(CH_3)_3$), 53.3 (C2'), 30.3 (C3'), 28.3 (OC($\underline{C}H_3)_3$), 27.9 (OC($\underline{C}H_3)_3$ – imidazole) + **DSG** part.

Analogue **8** — (25*R*)–spirost–5–en–3β–yl *N*–(*t*–butoxycarbonyl)–*L*–methioninate:

yield 98%, white solid, m.p. 121.9°C; $[M+H]^+$ calcd for $C_{37}H_{60}NO_6S$: 646.4141, found: 646.4149, $[M+Na]^+$ calcd for $C_{37}H_{59}NO_6SNa$: 668.3961, found: 668.3972.

^{1}H NMR δ [ppm]: *L*–methionine part: 5.12 (1H, d, *J* = 8.0 Hz), 4.36 (1H, m), 2.53 (2H, m), 2.33 (2H, m), 2.11 (3H, s, S–CH_3), 1.44 (9H, s, protons of *t*–Bu) + **DSG** part,

^{13}C NMR δ [ppm]: *L*–methionine part :171.6 (C1'), 155.3 (NH<u>C</u>O), 79.9 (O<u>C</u>$(CH_3)_3$), 32.4 and 30.0 (C3' and C4'), 28.3 (OC($\underline{C}H_3)_3$), 15.5 (CH_3–S) + **DSG** part.

Analogue **11** — (25*R*)–spirost–5–en–3β–yl *N*–(*t*–butoxycarbonyl)–*L*–alaninate:

yield 95%, white solid, m.p. 221.7°C; $[M+H]^+$ calcd for $C_{35}H_{56}NO_6$: 586.4108, found: 586.4105.

^{1}H NMR δ [ppm]: *L*–alanine part: 5.06 (1H, d, *J* = 6.6 Hz, NH), 4.26 (1H, m, H2'), 1.45 (9H, s, *t*–Bu), 1.37 (3H, d, *J* = 7.2 Hz, CH_3–3') + **DSG** part,

^{13}C NMR δ [ppm]: *L*–alanine part: 172.8 (C1'), 155.1 (NH<u>C</u>O), 79.7 (O<u>C</u>$(CH_3)_3$), 49.3 (C2'), 28.3 (OC($\underline{C}H_3)_3$), 18.8 (CH_3–3') + **DSG** part.

Analogue **12** — (25*R*)–spirost–5–en–3β–yl *N*–(*t*–butoxycarbonyl)–*L*–phenylalaninate:

yield 78%, white solid, m.p. 143.5°C; $[M+H]^+$ calcd for $C_{41}H_{60}NO_6$: 662.4421, found: 662.4422.

^{1}H NMR δ [ppm]: *L*–phenylalanine part: 7.29, 7.24, 7.15 (5H, m, Ph), 4.53 (1H, m, H2'), 3.07 (2H, m, H3'), 1.43 (9H, s, *t*–Bu) + **DSG** part,

^{13}C NMR δ [ppm]: *L*–phenylalanine part: 171.2 (C1'), 155.1 (NH<u>C</u>O), 136.1, 129.4, 128.4, 126.9 (Ph), 79.8 (O<u>C</u>$(CH_3)_3$), 54.5 (C2'), 38.4 (C3'), 28.3 (OC($\underline{C}H_3)_3$) + **DSG** part.

Analogue **13** — (25*R*)–spirost–5–en–3β–yl *N*–(*t*–butoxycarbonyl)–*L*–leucinate:

yield 78%, white solid, m.p. 150.9°C; $[M+H]^+$ calcd for $C_{38}H_{62}NO_6$: 628.4577, found: 628.4581, $[M+Na]^+$ calcd for $C_{38}H_{61}NO_6Na$: 650.4397, found: 650.4408.

^{1}H NMR δ [ppm]: *L*–leucine part: 4.89 (1H, d, *J* = 8.4 Hz, NH), 4.26 (1H, m, H2'), 1.71 (1H, m, H4'), 1.59 and 1.48 (both H3'), 1.44 (9H, s, *t*–Bu), 0.95 and 0.94 (2×3H, 2×CH_3 at C4') + **DSG** part,

^{13}C NMR δ [ppm]: *L*–leucine part: 172.9 (C1'), 155.4 (NH<u>C</u>O), 79.8 (O<u>C</u>$(CH_3)_3$), 52.2 (C2'), 41.9 (C3'), 28.3 (OC($\underline{C}H_3)_3$), 24.8 (C4'), 22.8 and 22.0 (both CH_3 groups at C4') + **DSG** part.

Analogue **14** — (25*R*)–spirost–5–en–3β–yl *N*–(*t*–butoxycarbonyl)–*L*–prolinate:

yield 94%, white solid, m.p. 185.4°C; $[M+H]^+$ calcd for $C_{37}H_{58}NO_6$: 612.4264, found: 612.4261, $[M+Na]^+$ calcd for $C_{37}H_{57}NO_6Na$: 634.4084, found: 634.4081.

NMR: mixture of two diasteroisomers **1**) and **2**) in the proportion 1.0 : 0.6.

^{1}H NMR δ [ppm]: *L*–proline part:

1) 4.19 (1H, m, H2'), 3.56 and 3.45 (2H, 2×m_{ov}, both H5'), 2.22 and 1.96 (2H, 2×m_{ov}, both H3'), 1.93 and 1.85 (2H, 2×m_{ov}, both H4'), 1.42 (9H, s, *t*–Bu) + **DSG** part,

2) 4.28 (1H, m, H2'), 3.51 and 3.38 (2H, 2×m_{ov}, both H5'), 2.18 and 1.94 (2H, 2×m_{ov}, both H3'), 1.94 and 1.87 (2H, 2×m_{ov}, both H4'), 1.46 (9H, s, *t*–Bu) + **DSG** part,

^{13}C NMR δ [ppm]: *L*–proline part:

1) 172.6 (C1'), 145.9 (NH<u>C</u>O), 79.8 (O<u>C</u>$(CH_3)_3$), 59.2 (C2'), 46.3 (C5'), 31.0 (C3'), 23.5 (C4'), 28.3 (OC($\underline{C}H_3)_3$) + **DSG** part,

2) 172.3 (C1'), 145.3 (NH<u>C</u>O), 79.6 (O<u>C</u>$(CH_3)_3$), 59.0 (C2'), 46.5 (C5'), 30.0 (C3'), 24.2 (C4'), 28.4 (OC($\underline{C}H_3)_3$) + **DSG** part.

Analogue **15** — (25*R*)–spirost–5–en–3β–yl levulinate:

yield 60%, white solid, m.p. 139.7°C; $[M+Na]^+$ calcd for $C_{32}H_{48}O_5Na$: 535.3399, found: 535.3395.

^{1}H NMR δ [ppm]: levulinic acid part: 2.74 (2H, t, H2'), 2.56 (2H, t, H3'), 2.20 (3H, s, CH_3–5') + **DSG** part,

^{13}C NMR δ [ppm]: levulinic acid part: 206.7 (C4'), 172.1 (C1'), 29.9 and 28.3 (C2' and C3') + **DSG** part.

Analogue **16** — (25*R*)–spirost–5–en–3β–yl (*E*)–3–(3,4–dialliloxyphenyl) acrylate:

yield 87%, white solid, m.p. 159.5°C; $[M+H]^+$ calcd for $C_{42}H_{57}O_6$: 657.4155, found: 657.4156, $[M+Na]^+$ calcd for $C_{42}H_{56}O_6Na$: 679.3975, found: 679.3975.

^{1}H NMR δ [ppm]: (*E*)–3–(3,4–dialliloxyphenyl)acrylic acid part: 7.58 (1H, d, *J* = 15.9 Hz, CH=CH *trans*), 7.07 (2H, m, two phenyl protons), 6.87 (1H, d, *J* = 8.5 Hz, one phenyl proton), 6.26 (1H, d, *J* = 15.9 Hz, CH=CH *trans*), 6.12 – 6.04 (2H, 2×m, both CH protons of CH_2=CH– groups), 5.45 and 5.41 (4H, 2×m, both CH_2 protons of CH_2=CH– groups), 4.64 (4H, m, both CH_2 protons of =CH–CH_2– groups) + **DSG** part,

^{13}C NMR δ [ppm]: (*E*)–3–(3,4–dialliloxyphenyl)acrylic acid part: 166.6, 150.5, 148.5, 144.3, 133.1, 132.9, 127.7, 122.4, 117.9, 117.8, 116.4, 113.4, 112.6, 69.9, 69.7 + **DSG** part.

*2.2.1.2. Synthesis of analogue **10** — (25R)–spirost–5–en–3β–yl N–(t–butoxycarbonyl)–L–isoleucyl–L–prolinate*

DIPEA (92 µL, 0.531 mM) was added to the solution of Boc–*L*–Ile–OH (41 mg, 0.177 mmol), TBTU (114 mg, 0.354 mmol) and HOBt (48 mg, 0,354 mmol) in DCM (5 mL) and the mixture was stirred for 15 min at room temperature. Then Boc–Pro–DSG **14** (150 mg, 0.274 mM) was added and the reaction mixture was stirred at room temperature for 24 h (TLC monitoring). After the reaction had been completed, DCM (15 mL) was added. The organic layer was washed successively with the aq. $NaHCO_3$ solution and then aq. NaCl solution. The extract was dried over anhydrous $MgSO_4$, filtered and evaporated to dryness. The crude product was purified through a silica gel column eluted with ethyl acetate–hexane.

Analogue **10** — (25*R*)–spirost–5–en–3β–yl *N*–(*t*–butoxycarbonyl)–*L*–isoleucyl–*L*–prolinate:

yield 94%, oil; $[M+H]^+$ calcd for $C_{43}H_{69}N_2O_7$: 725.5105, found: 725.5118.

^{1}H NMR δ [ppm]: *L*–isoleucine–*L*–proline part: 5.17 (1H, d, *J* = 9.4 Hz, NH at C7'), 4.47 (1H, m, H2'), 4.29 (1H, m, H7'), 3.82 (1H, m, one of H5') 3.66 (1H, m, one of H5'), 2.22 and 1.96 (2H, 2×m_{ov}, both H3'), 2.04 and 1.97 (2H, 2×m_{ov}, both H4'), 1.76 (1H, m, H8'), 1.60 and 1.14 (2H, both H9'), 1.42 (9H, s, *t*–Bu), 1.014 (3H, m, CH_3–at C8'), 0.90 (3H, m, CH_3–10') + **DSG** part,

^{13}C NMR δ [ppm]: *L*–isoleucine–*L*–proline part: 171.4 (C1'), 171.3 (C6'), 155.8 (NHCO), 79.4 (OC$(CH_3)_3$), 59.2 (C2'), 56.2 (C7'), 47.3 (C5'), 37.9 (C8'), 29.2 (C3'), 28.3 (OC(CH_3)$_3$), 24.9 (C4'), 24.2 (C9'), 15.3 (CH_3 at C8'), 11.2 (CH_3–10') + **DSG** part.

Analogue **9** — (25*R*)–spirost–5–en–3β–yl *N*–(*t*–butoxycarbonyl)–*L*–leucyl–*L*–valinate:

yield 97%, oil; $[M+H]^+$ calcd for $C_{43}H_{71}N_2O_7$: 727.5261, found: 727.5277, $[M+Na]^+$ calcd for $C_{43}H_{70}N_2O_7Na$: 749.5081, found: 749.5099.

^{1}H NMR δ [ppm]: *L*–leucine–*L*–valine part: 6.51 (1H, d, *J* = 8.8 Hz, NH, N3), 4.88 (1H, d, *J* = 7.3 Hz, NH at C5'), 4.49 (1H, dd, *J* = 4.8, 8.9 Hz, H2'), 4.12 (1H, m, H5'), 2.18 (1H, m, $(CH_3)_2$CH at C2'), 1.68 and 1.48 (both H6'), 1.60 (H7'), 1.44 (9H, s, *t*–Bu), 0.95 and 0.91 (12H, 4×CH_3, both CH_3 groups at C7'and both CH_3 groups $(CH_3)_2$CH at C2') + **DSG** part,

^{13}C NMR δ [ppm]: *L*–leucine–*L*–valine part: 172.3, 171.0 (C1' and C4'), 155.7 (NHCO), 80.0 (OC$(CH_3)_3$), 57.0 (C2'),53.1 (C5'), 40.9 (C6'), 31.4 (($CH_3)_2$CH at C2'), 24.8 (C7'), 22.8 and 22.2 (both CH_3 groups at C7'), 19.0 and 17.6 (both CH_3 groups of $(CH_3)_2$CH at C2') + **DSG** part.

*2.2.2 General procedure for the synthesis of compounds **2a**–**3a**, **5a**–**14a**, **16a***

2.2.2.1. Synthesis of (25R)–spirost–5–en–3β–yl O–benzyl–L–serinate hydrochloride.

Product **2** (112 mg, 0.162 mmol) was treated with 2.9M HCl/AcOEt (5.8 mM, 2 mL) and stirred for 24 h (TLC monitoring). The precipitated salt **2a** was collected by filtration and dried under vacuum at room temperature.

Analogue **2a** — (25*R*)–spirost–5–en–3β–yl *O*–benzyl–*L*–serinate hydrochloride:

yield 65%, m.p. 189.2°C; HRMS (ESI) m/z: $[M+H]^+$ calcd for $C_{37}H_{54}NO_5$: 592.4002, found: 592.4008.

^{1}H NMR δ [ppm] (CD_3OD): *O*–benzyl–*L*–serine: 7.35–7.30 (5H, phenyl), 4.66 (2H, d, *J* = 12.0 Hz, one of H5' protons), 4.53 (1H, d, *J* = 12.0 Hz, one of H5' protons), 4.25 (1H, dd, *J* = 3.1 and 3.8 Hz, H2'), 3.94 (1H, dd, *J* = 4.0 and 10.5 Hz, one of H3' protons), 3.83 (1H, dd, *J* = 3.0 and 10.5 Hz, one of H3' protons) + **DSG** part: 5.40 (1H, m, H6), 4.66 (1H, m, H3), 4.40 (1H, m, H16), 3.45 (1H, m, one of H27), 3.32 (m_{ov} with CH_3 from CD_3OD, one of H27), 2.28 (2H, m, both H4), 2.04 and 1.60 (both H7), 1.99 and 1.30 (both H15), 1.89 (H20), 1.93 and 1.15 (both H1), 1.90 and 1.66 (both H2), 1.78 and 1.22 (both H12), 1.75 (H17), 1.70 and 1.56 (both H23), 1.68 (H8), 1.62 and 1.42 (both H24), 1.60 (H25), 1.57 and 1.52 (both H11), 1.16 (H14), 1.06 (3H, s, CH_3–19), 0.97 (3H, d, *J* = 6.9 Hz, CH_3–21), 0.82 (3H, s, CH_3–18), 0.79 (3H, d, *J* = 6.5 Hz, CH_3–26),

^{13}C NMR δ [ppm]: *O*–benzyl–*L*–serine: 168.0 (C1'), [138.4, 129.6, 129.3, 129.2 – phenyl], 74.5 (C5'), 68.1 (C3'), 54.5 (C2') + **DSG** part: 140.5 (C5), 124.0 (C6), 110.6 (C22), 82.2 (C16), 77.9 (C3), 67.9 (C27), 63.8 (C17), 57.7 (C14), 51.5 (C9), 42.9 (C20), 41.4 (C13), 40.8 (C12), 38.9 (C4), 38.0 (C1), 37.9 (C10), 33.1 (C7), 32.7 (C15), 32.4 (C23), 31.4 (C25), 29.9 (C24), 28.5 (C2), 21.9 (C11), 19.7 (CH_3–19), 17.5 (CH_3–26), 16.8 (CH_3–18), 14.9 (CH_3–21).

Analogue **3a** — (25*R*)–spirost–5–en–3β–yl–*L*–isoleucinate hydrochloride:

yield 73%, m.p. 276.6°C (dec.); HRMS (ESI) m/z: $[M+H]^+$ calcd for $C_{33}H_{54}NO_4$: 528.4053, found: 528.4047.

^{1}H NMR δ [ppm] (CD_3OD): isoleucine part: 3.95 (1H, d, *J* = 4.0 Hz, H2'), 1.98 (1H, m, H3'), 1.56 and 1.38 (2H, both H4'), 1.04 (3H, d, *J* = 7.0 Hz, CH_3 at C3'), 1.01 (3H, t, *J* = 7.0 Hz, CH_3–5') + **DSG** part,

^{13}C NMR δ [ppm]: isoleucine: part: 169.3 (C1'), 58.3 (C2'), 37.9 (C3'), 26.8 (C4'), 14.9 (CH_3 at C3'), 12.0 (CH_3–5') + **DSG** part.

Analogue **5a** — (25*R*)–spirost–5–en–3β–yl–glycinate hydrochloride:

yield 65%; m.p. 242.7°C (dec.); HRMS (ESI) m/z: $[M+Na]^+$ calcd for $C_{29}H_{45}NO_4Na$: 494.3246, found: 494.3246.

^{1}H NMR δ [ppm] (CD_3OD): glycine part: 3.81 (2H, s, H2') + **DSG** part,

^{13}C NMR δ [ppm]: glycine part:168.0 (C1'), 41.2 (C2') + **DSG** part.

Analogue **6a** — (25*R*)–spirost–5–en–3β–yl–*L*–valinate hydrochloride:

yield 80%; m.p. 284.3°C (dec.); HRMS (ESI) m/z: $[M+H]^+$ calcd for $C_{32}H_{52}NO_4$: 514.3896, found: 514.3889.

^{1}H NMR δ [ppm]: valine part: 3.88 (1H, d, *J* = 4.5 Hz, H2'), 2.29 (1H, m, H3'), 1.09 and 1.08 (6H, 2×d_{ov}, both CH_3 groups at C3') + **DSG** part,

^{13}C NMR δ [ppm]: valine part: 169.4 (C1'), 59.4 (C2'), 31.0(C3'), 18.4 and 18.2 (both CH_3 groups at C3') + **DSG** part.

Analogue **7a** — (24*R*)–spirost–5–en–3β–yl–*L*–histidinate hydrochloride:

yield 87%; m.p. 227.5°C (dec.); HRMS (ESI) m/z: $[M+H]^+$ calcd for $C_{33}H_{50}N_3O_4$: 552.3801, found: 552.3799

^{1}H NMR δ [ppm] (CD_3OD): histidine part: 8.96 (1H, s, H6' – proton between both nitrogens in diazole ring), 7.56 (1H, s, H8'), 4.43 (1H, m_{ov}, H2'), 3.50 – 3.36 (2H, 2×m_{ov}, both H3') + **DSG** part,

^{13}C NMR δ [ppm]: histidine part: 168.4 (C1'), 135.9, 128.6, 119.7 – diazol ring, 53.0 (C2'), 26.7 (C3') + **DSG** part.

Analogue **8a** — (25*R*)–spirost–5–en–3β–yl–*L*–methioninate hydrochloride:

yield 77%; m.p. 253.3°C (dec.); HRMS (ESI) m/z: $[M+H]^+$ calcd for $C_{32}H_{52}NO_4S$: 546.3617, found: 546.3620.

^{1}H NMR δ [ppm] (CD_3OD): methionine part: 4.17 (1H, t, *J* = 6.4 Hz, H2'), 2.66 (2H, m, both H4'), 2.23 (1H, m, one of H3') and 2.14 (1H, m, one of H3'), 2.13 (3H, s, CH_3 at S) + **DSG** part,

^{13}C NMR δ [ppm]: methionine part: 169.8 (C1'), 52.9 (C2'), 30.8 (C3'), 30.1 (C4') 15.0 (CH_3 at S) + **DSG** part.

Analogue **9a** — (25*R*)–spirost–5–en–3β–yl–*L*–leucyl–*L*–valinate hydrochloride:

yield 63%; m.p. 228.4°C (dec.); HRMS (ESI) m/z: [M–H] calcd for $C_{38}H_{62}N_2O_5Cl$: 661.4347, found: 661.4343.

^{1}H NMR δ [ppm] (CD_3OD): *L*–leucine–*L*–valine part: 4.31 (1H, d, *J* = 5.9 Hz, H2'), 2.19 (1H, m, C<u>H</u>–$(CH_3)_2$ at C2'), 1.002 and 1.006 (both CH_3 groups of CH–(C<u>H</u>$_3)_2$ at C2'), 3.98 (1H, dd, *J*= 5.6 and 8.4 Hz, H5'), 1.75 (2H, one of H6'and H7'), 1.67 (1H, one of H6'), 1.022 and 1.008 (both CH_3 groups at C7') + **DSG** part,

^{13}C NMR δ [ppm] (CD_3OD): *L*–leucine–*L*–valine part: 171.8 (C1'), 171.0 (C4'), 59.8 (C2'), 52.8 (C5'), 41.9 (C6'), 25.3 (C7'), 31.5 (<u>C</u>H–$(CH_3)_2$ at C2'), 23.2 and 22.2 (both CH_3 groups at C7'), 19.4 and 18.6 (both CH_3 groups of CH–(<u>C</u>$H_3)_2$ at C2') + **DSG** part.

Analogue **10a** — (25*R*)–spirost–5–en–3β–yl–*L*–isoleucyl–*L*–prolinate hydrochloride:

yield 70%; m.p. 210.3°C (dec.); HRMS (ESI) m/z: $[M+H]^+$ calcd for $C_{38}H_{61}N_2O_5$: 625.4580, found: 625.4568.

^{1}H NMR δ [ppm] (CD_3OD): 4.48 (1H, m, H2'), 4.10 (1H, d, *J* = 5.6 Hz, H7'), 3.76 (1H, m, one of H5'), 3.63 (1H, m, one of H5'), 2.32 and 1.97 (both H3'), 2.07 and 2.01 (both H4' and H8'), 1.66 and 1.25 (both H9'), 1.14 (CH_3 at C8'), 1.00 (CH_3–10') + **DSG** part,

^{13}C NMR δ [ppm] (CD_3OD): 172.5 (C1'), 168.6 (C6'), 61.0 (C2'), 57.7 (C7'), 48.9 (C5'), 37.6 (C8'), 30.2 (C3'), 26.2 (C4'), 24.7 (C9'), 15.1 (CH_3 at C8'), 11.7 (CH_3–10') + **DSG** part.

Analogue **11a** — (25*R*)–spirost–5–en–3β–yl–*L*–alaninate hydrochloride:

yield 92%; m.p. 275.4°C (dec.); HRMS (ESI) m/z: $[M+H]^+$ calcd for $C_{30}H_{48}NO_4$: 486.3583, found: 486.3581.

^{1}H NMR δ [ppm] (CD_3OD): *L*–alanine part: 4.04 (1H, q, *J* = 7.2 Hz, H2'), 1.52 (3H, d, *J* = 7.2 Hz, CH_3–3') + **DSG** part,

^{13}C NMR δ [ppm] (CD_3OD): *L*–alanine part: 170.5 (C1'), 49.9 (C2'), 16.3 (CH_3–3') + **DSG** part.

Analogue **12a** — (25*R*)–spirost–5–en–3β–yl–*L*–phenylalaninate hydrochloride:

yield 93%; m.p. 253.0°C (dec.); HRMS (ESI) m/z: $[M+H]^+$ calcd for $C_{36}H_{52}NO_4$: 562.3896, found: 562.3892.

^{1}H NMR δ [ppm] (CD_3OD): *L*–phenylalanine part: 7.33 – 7.28 (5H, m, phenyl), 4.27 (1H, t, *J* = 7.1 Hz, H2'), 3.21 (2H, m, both H3') + **DSG** part.

^{13}C NMR δ [ppm] (CD_3OD): *L*–phenylalanine part: 169.5 (C1'), 135.4, 130.6, 130.1, 128.9 – phenyl, 55.2 (C2'), 37.7 (C3') + **DSG** part.

Analogue **13a** — (25*R*)–spirost–5–en–3β–yl–*L*–leucinate hydrochloride:

yield 84%; m.p. 263.8°C (dec.); HRMS (ESI) m/z: $[M+H]^+$ calcd for $C_{33}H_{54}NO_4$: 528.4053, found: 528.4047.

^{1}H NMR δ [ppm] (CD_3OD): *L*–leucine part: 3.98 (1H, m, H2'), 1.79 (1H, m_{ov}, H4'), 1.80 and 1.68 (2H, 2×m_{ov}, both H3'), 1.02 and 1.00 (2×3H, both CH_3 groups at C4') + **DSG** part.

^{13}C NMR δ [ppm] (CD_3OD): *L*–leucine part: 170.4 (C1'), 52.6 (C2'), 40.9 (C3'), 25.7 (C4'), 22.6 and 22.4 (both CH_3 groups at C4') + **DSG** part.

Analogue **14a** — (25*R*)–spirost–5–en–3β–yl–*L*–prolinate hydrochloride:

yield 74%; m.p. 249.8°C (dec.); HRMS (ESI) m/z: $[M+H]^+$ calcd for $C_{32}H_{50}NO_4$: 512.3740, found: 512.3733.

^{1}H NMR δ [ppm] (CD_3OD): *L*–proline: 4.41 (1H, m, H2'), 3.38 (2H, m_{ov}, H5'), 2.08 (2H, m, H4'), 2.43 and 2.12 (2H, 2×m_{ov}, H3') + **DSG** part.

^{13}C NMR δ [ppm] (CD_3OD): *L*–proline: 169.6 (C1'), 60.8 (C2'), 47.2 (C5'), 29.5 (C3'), 24.5 (C4') + **DSG** part.

2.2.2.2 (25R)–spirost–5–en–3β–yl (E)–3–(3,4–dihydroxyphenyl)acrylate

1,3–dimethylbarbituric acid (1.5 g, 9.608 mM), Ph_3P (296 mg, 1.129 mM) and $Pd(OAc)_2$ (299 mg, 1.333 mM) were added to the suspension of DSG–*O*–caff–All (**16**) (700 mg, 1.066 mM) in EtOH (53 mL). The reaction mixture was heated to 75°C for 3 hours. After the reaction had been completed (TLC control), the mixture was filtered through a cellite pad and the filtrate was evaporated under reduced pressure. DCM was added and washed with 5% aq. $NaHCO_3$ and water. The extract was dried over anhydrous $MgSO_4$, filtered and evaporated to dryness. The crude product was purified through a silica gel column eluted with DCM/MeOH (95:5) (v/v) to give a white solid.

Analogue **16a** — (25*R*)–spirost–5–en–3β–yl (*E*)–3–(3,4–dihydroxyphenyl)acrylate:

yield 98%, m.p. 218.4°C (dec.); HRMS (ESI) m/z: [M–H] calcd for $C_{36}H_{47}O_6$: 575.3373, found: 575.3369.

^{1}H NMR δ [ppm]: (*E*)–3–(3,4–dihydroxyphenyl)acrylic acid part: 7.57 (1H, d, *J* = 15.9 Hz, H2'), 7.11 (1H, d, *J* = 1.8 Hz, H5'), 6.99 (1H, dd, *J* = 1.8 and 8.4 Hz, H9'), 6.87 (1H, d, *J* = 8.4 Hz, H8'), 6.56 (1H, br, OH), 6.43 (1H, br, OH), 6.24 (1H, d, *J* = 15.9 Hz, H3') + **DSG** part,

^{13}C NMR δ [ppm]: (*E*)–3–(3,4–dihydroxyphenyl)acrylic acid part: 167.4 (C1'), (146.6, 145.0, 144.1, 127.4, 122.3, 115.8, 115.4, 114.3 – phenyl and double bond carbons) + **DSG** part.

*2.2.3.Synthesis of compounds **2b** and **4b***

(25*R*)–5α–spirostan–3β–yl *N*–(*t*–butoxycarbonyl)–*L*–serinate **2b**:

A solution of **2** (290 mg, 0.419 mmol) in 20 ml AcOEt was hydrogenated in the presence of 10% palladium on charcoal (70 mg) for 6 hrs. After filtration through a cellite pad, the solution was evaporated. The product was obtained as a white solid, yield 199 mg (79%).

Analogue **2b** — (25*R*)–5α–spirostan–3β–yl *N*–(*t*–butoxycarbonyl)–*L*–serinate:

yield 79%, m.p. 214.9°C; $[M+H]^+$ calcd for $C_{35}H_{58}NO_7$: 604.4213, found: 604.4218, $[M+Na]^+$ calcd for $C_{35}H_{57}NO_7Na$: 626.4033, found: 626.4041.

^{1}H NMR δ [ppm]: *L*–serine part: 5.46 (1H, d, *J* = 6.4 Hz, NH), 4.29 (1H, m, H1'), 3.89 (2H, m, both H3'), 1.43 (9H, s, *t*–Bu); **TGG** part: 4.75 (1H, m, H3), 4.36 (1H, m, H16), 3.44 (1H, ddd, *J* = 2.0, 4.1, 10.9 Hz, one of H27), 3.36 (1H, t, *J* = 10.9 Hz, one of H27), 1.83 (H20), 1.73 (H17), 1.59 (H25), 1.51 (H8), 1.14 (H5), 1.07 (H14), 0.64 (H9), 1.67 and 1.10 (both H12), 1.71 and 1.00 (both H1), 1.59 and 1.36 (both H4), 1.65 and 0.87 (both H7), 1.95 and 1.22 (both H15), 1.64 and 1.56 (both H23), 1.59

and 1.42 (both H24), 1.25 (both H6), 1.81 and 1.51 (both H2), 1.47 and 1.26 (both H11), 0.93 (3H, d, *J* = 7.0 Hz, CH_3–21), 0.81 (3H, s, CH_3–19), 0.76 (3H, d, *J* = 6.4 Hz, CH_3–26), 0.73 (3H, s, CH_3–18),

^{13}C NMR δ [ppm]: *L*–serine part: 170.2 (C1'), 155.8 (O<u>C</u>OC(CH_3)$_3$), 80.2 (OCO<u>C</u>(CH_3)$_3$), 55.9 (C2'), 63.8 (C3'), 28.3 (OCOC(<u>C</u>H_3)$_3$); **TGG** part: 109.2 (C22), 80.8 (C16), 75.4 (C3), 66.8 (C27), 62.1 (C17), 56.2 (C14), 54.1 (C9), 44.6 (C5), 41.6 (C20), 40.5 (C13), 40.0 (C12), 36.6 (C1), 35.5 (C10), 35.0 (C8), 33.8 (C4), 32.1 (C7), 31.7 (C15), 31.3 (C23), 30.3 (C25), 28.8 (C24), 28.4 (C6), 27.3 (C2), 21.0 (C11), 17.1 (CH_3–26), 16.4 (CH_3–18), 14.5 (CH_3–21), 12.2 (CH_3–19).

Analogue **4b** — (25*R*)–5α–spirostan–3β–yl *N*–(*t*–butoxycarbonyl)–*L*–glutamate:

yield 94%, m.p. 183.2°C; $[M+H]^+$ calcd for $C_{37}H_{60}NO_8$: 646.4319, found: 646.4323, $[M+Na]^+$ calcd for $C_{37}H_{59}NO_8Na$: 668.4138, found: 668.4143.

^{1}H NMR δ [ppm]: *L*–glutamic acid part: 5.17 (1H, d, *J* = 8.0 Hz, NH), 4.28 (1H, m, H2'), 2.44 (2H, m, both H4'), 2.17 and 1.92 (2H, 2×m_{ov}, both H3'), 1.43 (9H, s, *t*–Bu); **TGG** part: 4.74 (1H, m, H3), 4.39 (1H, m, H16), 3.46 (1H, ddd, *J* = 2.0, 4.1, 10.9 Hz, one of H27), 3.36 (1H, t, *J* = 10.9 Hz, one of H27), 1.85 (H20), 1.75 (H17), 1.61 (H25), 1.52 (H8), 1.15 (H5), 1.09 (H14), 0.65 (H9), 1.69 and 1.12 (both H12), 1.72 and 1.00 (both H1), 1.57 and 1.37 (both H4), 1.66 and 0.89 (both H7), 1.97 and 1.24 (both H15), 1.66 and 1.58 (both H23), 1.60 and 1.43 (both H24), 1.27 (both H6), 1.80 and 1.52 (both H2), 1.48 and 1.28 (both H11), 0.95 (3H, d, *J* = 7.0 Hz, CH_3–21), 0.83 (3H, s, CH_3–19), 0.78 (3H, d, *J* = 6.4 Hz, CH_3–26), 0.75 (3H, s, CH_3–18),

^{13}C NMR δ [ppm]: *L*–glutamic acid part: 177.2 (CO–5'), 171.6 (CO–1'), 155.6 (O<u>C</u>OC(CH_3)$_3$), 80.2 (OCO<u>C</u>(CH_3)$_3$), 52.9 (C2'), 30.1 (C4') 28.7 (C3'), 28.3 (OCOC(<u>C</u>H_3)$_3$); **TGG** part: 109.3 (C22), 80.8 (C16), 75.2 (C3), 66.9 (C27), 62.2 (C17), 56.2 (C14), 54.2 (C9), 44.6 (C5), 41.6 (C20), 40.6 (C13), 40.0 (C12), 36.6 (C1), 35.6 (C10), 35.1 (C8), 33.8 (C4), 32.1 (C7), 31.8 (C15), 30.3 (C25), 28.8 (C24), 28.5 (C6), 27.4 (C2), 21.0 (C11), 17.1 (CH_3–26), 16.5 (CH_3–18), 14.5 (CH_3–21), 12.3 (CH_3–19).

*2.2.4.Synthesis of compounds **2c** and **4c***

Synthesis of (25*R*)–5α–spirostan–3β–yl *L*–serinate hydrochloride **2c**:

Product **2b** (96 mg, 0.159 mmol) was treated with 2.9M HCl/AcOEt (8.7 mM, 3 mL) and stirred for 24 h (TLC monitoring). The precipitated salt was collected by filtration and dried under vacuum at room temperature.

Analogue **2c**— (25*R*)–5α–spirostan–3β–yl *L*–serinate hydrochloride:

yield 98%, m.p. 241.5°C (dec.); HRMS (ESI) m/z: $[M+H]^+$ calcd for $C_{30}H_{50}NO_5$: 504.3689, found: 504.3688.

^{1}H NMR δ [ppm] (CD_3OD): *L*–serine part: 4.06 (1H, m, H2'), 3.97 (1H, dd, *J* = 4.8 and 11.7 Hz, one of H2'), 3.92 (1H, dd, *J* = 3.5 and 11.7 Hz, one of H2'), **TGG** part: 4.84 (H3), 4.38 (H16), 3.45 and 3.32 (2H, 2×m, both H27), 1.90 (H20), 1.74 (H17), 1.61 (H8), 1.60 (H25), 1.23 (H5), 1.16 (H14), 0.74 (H9), 1.98 and 1.26 (both H15), 1.90 and 1.61 (both H2), 1.80 and 1.08 (both H1), 1.73 and 0.97 (both H7), 1.66 and 1.48 (both H4), 1.74 and 1.17 (both H12), 1.70 and 1.56 (both H23), 1.63 and 1.42 (both H24), 1.55 and 1.36 (both H11), 1.33 (both H6), 0.96 (CH_3–21), 0.90 (CH_3–19), 0.80 (CH_3–18), 0.79 (CH_3–26), 0.74 (H9),

^{13}C NMR δ [ppm] (CD_3OD): *L*–serine part: 168.4 (C1'), 60.7 (C3'), 56.1 (C2'), **TGG** part: 110.6 (C22), 82.2 (C16), 77.7 (C3), 67.9 (C27), 63.8 (C17), 57.5 (C14), 55.6 (C9), 45.9 (C5), 42.9 (C20), 41.7 (C13), 41.1 (C12), 37.8 (C1), 36.7 (C10), 36.5 (C8), 34.8 (C4), 33.3 (C7), 32.6 (C15), 32.4 (C23), 31.4 (C25), 29.9 (C24), 29.6 (C6), 28.4 (C2), 22.1 (C11), 17.5 (CH_3–26), 16.9 (CH_3–18), 14.9 (CH_3–21), 12.6 (CH_3–19).

Analogue **4c**— (25*R*)–5α–spirostan–3β–yl *L*–glutamate hydrochloride:

yield 65%, m.p. 212°C; HRMS (ESI) m/z: $[M+H]^+$ calcd for $C_{32}H_{52}NO_6$: 546.3795, found: 546.3791.

^{1}H NMR δ [ppm] (CD_3OD): *L*–glutamic acid part: 4.06 (1H, t, *J* = 6.8 Hz, H2'), 2.15 (2H, m, both H3'), 2.53 (2H, m, both H4') + **TGG** part,

^{13}C NMR δ [ppm] (CD_3OD): *L*–glutamic acid part: 175.4 (C5'), 169.7 (C1'), 53.4 (C2'), 30.3 (C4'), 26.7 (C3') + **TGG** part.

*2.2.5.Synthesis of compounds **17** and **18***

*2.2.5.1. Synthesis of (25R)–spirost–5–en–3β–yl acetate **17***

Acetic anhydride (0.7 ml, 7.42 mmol) was added to the solution of diosgenin (2 g, 4.82 mmol), DMAP (0.6 g, 4.91 mmol) and TEA (6.4 ml, 45.98 mmol) in DCM (100 ml) at room temperature. The solution was stirred at room temperature for 24 h. After the reaction had been completed (TLC control), the organic layer was washed successively with water (90 ml) and a saturated aq. $NaHCO_3$ solution (80 ml). The extract was dried over anhydrous $MgSO_4$, filtered and evaporated to dryness. The crude product was crystallized from ethyl acetate to afford a white solid.

Analogue **17** — (25*R*)–spirost–5–en–3β–yl acetate:

yield 83%, m.p. 204.7°C; $[M+H]^+$ calcd for $C_{29}H_{45}O_4$: 457.3318, found: 457.3323.

^{1}H NMR δ [ppm]: 2.03 (3H, s, CH_3 of C$\underline{H}_3$CO at C3) + **DSG** part: 5.38 (1H, m, H6), 4.60 (1H, m, H3), 4.41 (1H, m, H16), 3.47 (1H, ddd, *J* = 2.3, 4.3 and 10.9 Hz, one of H27), 3.38 (1H, t, *J* = 11.0 Hz, one of H27), 2.32 (2H, m_{ov}, both H4), 2.00 and 1.56 (m_{ov},both H7), 1.98 and 1.29 (m_{ov},both H15), 1.87 (1H, m_{ov}, H20), 1.86 and 1.58 (m_{ov}, both H2), 1.86 and 1.13 (m_{ov},both H1), 1.78 (1H, m_{ov}, H17), 1.74 and 1.19 (m_{ov}, both H12), 1.68 and 1.59 (m_{ov}, both H23), 1.63 (2H, m_{ov}, H8 and H25), 1.62 and 1.45 (m_{ov}, both H24), 1.51 and 1.46 (m_{ov}, both H11), 1.12 (1H, m_{ov}, H14), 1.04 (3H, s, CH_3–19), 0.98 (1H, m_{ov}, H9), 0.97 (3H, d, *J* = 6.8 Hz, CH_3–21), 0.79 (6H, 2×d_{ov} CH_3–25 and CH_3–18),

^{13}C NMR δ [ppm]: 170.5 (C1'), 21.4 (CH_3 of C$\underline{H}_3$CO at C3) + **DSG** part: 139.7 (C5), 122.3 (C6), 109.3 (C22), 80.8 (C16), 73.9 (C3), 66.8 (C27), 62.1 (C17), 56.4 (C14), 49.9 (C9), 41.6 (C20), 40.2 (C13), 39.7 (C12), 38.1 (C4), 36.9 (C1), 36.7 (C10), 32.0 (C7), 31.8 (C15), 31.4 (C23 and C8), 30.3 (C25), 28.8 (C24), 27.7 (C2), 20.8 (C11), 19.3 (C19), 17.1 (C26), 16.3 (C18), 14.5 (C21).

*2.2.5.2.Synthesis of (25R)–furost–5–en–3β–acetoxy–26–ol **18***

DSG–3–acetate (1 g, 2.19 mmol) was dissolved in acetic anhydride (70 ml) at room temperature, and then sodium cyanoborohydride (1 g, 15.91 mmol) was added in portions over a period of 30 min. This mixture was stirred for 3 h at room temperature (TLC control). Then, the reaction was poured into ice–cold water (450 ml), extracted with AcOEt (3×70 ml), and washed with water. The extract was dried over anhydrous $MgSO_4$, filtered and evaporated to dryness. The crude product was purified through a silica gel column with hexane–ethyl acetate.

Analogue **18** — (25*R*)–furost–5–en–3β–acetoxy–26–ol:

yield 98%, m.p. 107.4°C; HRMS (ESI) m/z: $[M+Na]^+$ calcd for $C_{29}H_{46}O_4Na$: 481.3294, found: 481.3296.

^{1}H NMR δ [ppm]: 2.03 (3H, s, CH_3CO– at C3) + **DSG** part: 5.37 (1H, m, H6), 4.60 (1H, m, H3), 4.31 (1H, m, H16), 3.50 and 3.44 (2H, 2×dd, *J* = 6.2, 10.7 Hz, both H27), 3.33 (1H, m, H22), 2.32 (2H, m, both H4), , 2.00 and 1.31 (2×m_{ov}, both H15), 1.99 and 1.54 (2×m_{ov}, both H7), 1.86 and 1.59 (2×m_{ov}, both H2), 1.86 and 1.14 (2×m_{ov}, both H1), 1.75 (m, H20), 1.72 and 1.13 (2×m_{ov}, both H12), 1.67 (m_{ov}, H25), 1.62 (m_{ov}, H8), 1.60 (m_{ov}, H17), 1.59 (m_{ov}, both H23), 1.51 and 1.45 (2×m_{ov}, both H11), 1.47 and 1.35 (2×m_{ov}, both H24), 1.09 (1H, m_{ov}, H14), 1.03 (3H, s, CH_3–19), 1.00 (3H, d, *J* = 6.7 Hz, CH_3–21), 0.95 (1H, m_{ov}, H9), 0.91 (3H, d, *J* = 6.8 Hz, CH_3–27), 0.81 (3H, s, CH_3–18),

^{13}C NMR δ [ppm]: 170.5 (CO at C3), 21.4 (CH_3CO at C3) + **DSG** part: 139.7 (C5), 122.4 (C6), 90.3 (C22), 83.2 (C16), 73.9 (C3), 68.1 (C27), 65.1 (C17), 56.9 (C14), 50.0 (C9), 40.7 (C13), 39.4 (C12), 38.1 (C4), 37.9 (C20), 37.0 (C1), 36.7 (C10), 35.7 (C25), 32.2 (C15), 32.0 (C7), 31.5 (C8), 30.4 (C23), 30.1 (C24), 27.7 (C2), 20.6 (C11), 19.3 (CH_3–19), 18.9 (CH_3–21), 16.6 (CH_3–26), 16.4 (CH_3–18).

2.3. Biological studies

2.3.1. Cells and a cytotoxicity assay

Human umbilical vein endothelial cells (HUVEC, purchased from Life Technologies, Carlsbad, CA, USA) were cultured in the Medium 200 with a low serum growth supplement (Life Technologies Carlsbad, CA, USA) according to the manufacturer's instructions. The MCF–7 cells (mammary gland, breast; derived from the metastatic site) were cultivated in the Eagle's Minimum Essential Medium supplemented with 1% non–essential amino acids. PC–3 cells (prostate; derived from the metastatic site: bone) were cultured in the RPMI 1640 medium (Gibco, Thermo Fisher Scientific, Waltham, MA, USA). MDA–MB–231 cells (mammary gland) were cultured in the DMEM (Gibco, Thermo Fisher Scientific, Waltham, MA, USA medium). THP–1 cells (human monocytic leukemia) were grown in RPMI 1640 supplemented with 0.05 mM β–mercaptoethanol (Sigma, St. Louis, MO, USA). All cell culture media were supplemented with a 10% fetal bovine serum FBS (Gibco, Thermo Fisher Scientific, Waltham, MA, USA) and antibiotics. The cells were grown at 37°C in a 5% CO_2 atmosphere.

For the cytotoxicity studies 10×10^3 cells/well of HUVEC or 7×10^3 cells/well of cancer cells were seeded on a 96–well plate (Nunc, Roskilde, Denmark). 24 hours later the cells were exposed to the test compounds for additional 48 hours. Stock solutions of the test compounds were freshly prepared in ethanol. The final concentrations of the compounds tested in the cell cultures were: 1×10^{-1} mM, 4×10^{-2} mM, 1.6×10^{-2} mM, 6.5×10^{-3} mM, 2.5×10^{-3} mM and 1×10^{-3} mM. The concentration of ethanol in the cell culture medium was 1%.

The IC_{50} values were calculated from dose–response curves and used as a measure of cellular sensitivity to a given treatment.

The cytotoxicity of all compounds was determined by the MTT [3–(4,5–dimethylthiazol–2–yl)–2,5–diphenyltetrazolium bromide; Sigma, St. Louis, MO] assay as described [27]. Briefly, after 24 or 48 hours of incubation with drugs, the cells were treated with the MTT reagent and the incubation was continued for 2 hours. MTT–formazan crystals were dissolved in 20% SDS and 50% DMF at pH 4.7 and the absorbance was read at 570 and 650 nm on the ELISA–PLATE READER (FLUOstar Omega). As control (100% viability), we used cells grown in the presence of a vehicle (1% Ethanol) only.

2.3.2. Caspase-3/7 enzymatic activity assay

MCF–7 cells were cultured in the Eagle's Minimum Essential Medium supplemented with antibiotics and a 10% fetal bovine serum in a 5% CO_2 atmosphere at 37°C. 20×10^3 cells were seeded in each well on a 96–well plate (Nunc, Roskilde, Denmark). After 24 hours the cells were exposed to the test compound **2c** at the concentration of $2\times IC_{50}$ and $5\times IC_{50}$ for another 18 hours. The cells were also exposed to 1% ethanol (vehicle control) or 1μM staurosporine (a strong inducer of cell apoptosis, Sigma, St. Louis, MO). The induction of cell apoptosis was analyzed by the Apo–ONE® Homogeneous Caspase–3/7 Assay (Promega, Madison, WI, USA). After 18 hours of incubation with the test compounds, the cells were treated with the caspase–3/7 reagent according to the manufacturer's instructions and incubated for additional 1.5 hour at room temperature. The fluorescence in each well was measured in triplicate (excitation at 485 nm, emission measured at 520 nm) using a microplate reader FLUOStar Omega (BMG–Labtech, Germany). For the normalization of data, the level of caspase activation in the control cells (exposed to 1% ethanol) was taken as 1.0.

2.3.3.Cytokine mRNA quantification by real–time RT–PCR

A real–time RT–PCR method was used to measure the mRNA level of a given cytokine (IL–1, IL–4, IL–10, IL–12, TNF–α) in THP–1 cells (Institute of Medical Biology of Polish Academy of Sciences, Łódź, Poland) exposed to diosgenin or its derivatives. To obtain RNA for the gene expression analysis, THP–1 cells were seeded on a 6–well plate (Nunc) in the amount of 1×10^6 cells/well and exposed to the test compounds at the concentration of 5 μM for another 6 hours. The control cells were exposed to 1% ethanol or 5 μg/ml LPS (Sigma, St. Louis, MO, USA). The total RNA pool was isolated from the cell lysates using a TriPure Isolation Reagent (Roche, Basel, Switzerland) according to the manufacturer's instruction. The RNA purity and integrity were checked spectrophotometrically with a NanoDrop ND–1000 spectrophotometer (Thermo Fisher Scientific).

Reverse transcription and PCR amplification reactions were performed in one step using the LightCycler® 1.0 Instrument (Roche) and LightCycler RNA Amplification Kit SYBR Green I (Roche). Each sample contained 250 ng of total RNA, 2 mM $MgCl_2$, 2 μl of 5x SYBR Green, 0.25 μM of forward and reverse primers, and 0.2 μl of the enzyme mix (total sample volume of 10 μl). The qRT–PCR reactions were optimized for each studied gene and performed according to a general protocol: a reverse transcription reaction (RT) for 10 minutes at 55°C, and a denaturation step for 30 seconds at 95°C. Three steps of the PCR quantification reaction included: I – denaturation (0 seconds at 95°C), II – annealing (10 seconds at 61°C), III – product extension (8 seconds at 72°C), 45 cycles in total. Subsequent melting experiments were performed by quick denaturation at 95ºC, annealing over 10 seconds at 65°C and heating up to 95°C at 0.1 C/s. The IL–1, IL–4, IL–10, IL–12, and the TNF–α mRNA levels were normalized against the reference GAPDH mRNA. Changes in the mRNA expression invoked by the tested compounds were calculated using the ΔΔCt method (calibrator–RNA isolated from THP–1 cells exposed to 1% ethanol, mean values ± standard deviation from three experiments are given). Primer sequences for the real–time RT–PCR reactions were taken from literature data [28].

Table 1. Primers used for the amplification of cytokine mRNA (IL–1, IL–4, IL–10, IL–12, TNF–α) and GAPDH in real–time RT–PCR reaction.

mRNA	Sequence	
IL–1	Fwd	5'–CCTGTCCTGCGTGTTGAAAGA–3'
	Rev	5'–GGGAACTGGGCAGACTCAAA–3'
IL–4	Fwd	5'–AACAGCCTCACAGAGCAGAAGAC–3'
	Rev	5'–GCCCTGCAGAAGGTTTCCTT–3'
IL–10	Fwd	5'–GCTGGAGGACTTTAAGGGTTACCT–3'
	Rev	5'–CTTGATGTCTGGGTCTTGGTTCT–3'
IL–12	Fwd	5'–CATGGTGGATGCCGTTCA–3'
	Rev	5'–ACCTCCACCTGCCGAGAAT–3'
TNF–α	Fwd	5'–CCCCAGGGACCTCTCTCTAATC–3'
	Rev	5'–GGTTTGCTACAACATGGGCTACA–3'
GADPH	Fwd	5'–CATCATCTCTGCCCCCTCTC–3'
	Rev	5'–CTGTTGAAACCATAGCACCT–3'

2.4. Statistical analysis

The results were subjected to a nonparametric analysis of the ANOVA variance followed by the Tukey *post–hoc* test. The analyzes were performed using the GraphPad_Prism 8 program (GraphPad Software Inc., USA). As a borderline level of significance, $p < 0.05$ was accepted.

2.5. Computational methods

In the computational part of this work we first built the models of all studied molecules manually and then the LigProp 3.3 software (Schrodinger Inc.) was used to prepare all atom 3D structures. Afterwards, we evaluated all ADME properties using the QikProp 4.6 software (Schrodinger Inc.) with default options. The most important selected ADME properties have been presented in Table 4 and analyzed in section 3.4.

2.6. Molecular docking

For the molecular docking part we used the crystal structure (PDB code: 2YAT [29]) of the estrogen receptor–ligand binding domain complex and the crystal structure (PDB code: 4UDD [30]) of the GR. The ligand and water molecules were removed, which was followed by the addition of hydrogen atoms with AutoDockTools 4 [31]. Atomic interaction energy grids were calculated using probes corresponding to each atomic type found in the **2c** molecule at the 0.375 Å grid resolution. In all docking experiments all ligands were treated in a fully flexible manner with the Gasteiger partial charges added by AutoDockTools 4. For each ligand–receptor pair we used a two–step docking protocol to assess the most likely binding site of the ligands in the receptors. In the first step we used a 116×126×126 (2YAT) or 126×126×126 (4UDD) Å cubic boxes that spanned over all the receptors and as amino acids were treated as rigid. We used Autodock 4.2 [31] with the Genetic Lamarckian Algorithm and standard options, but including 200 dockings per compound and 5,000,000 energy evaluations per docking [32]. Such an approach allowed us to identify three potential binding sites within the estrogen receptor with relatively low estimates of **2c** binding affinities (<220 nM) and three binding sites within the GR with low estimates of **4c** and **16a** binding affinities (<70 nM). In the second step a more accurate docking to these potential sites was performed using the same docking protocol. However, the selected amino acids were treated as flexible (see Table 2) and docked to smaller, better defined sites.

Table 2. List of flexible residues

Potential binding site	List of flexible residues
2YAT site 1	GLU353, ARG394, PHE404, GLU423, PHE425, HIS524
2YAT site 2	GLU423, ASP426, ARG434, HIS513
2YAT site 3	SER381, THR460, ARG515, ASN519, ARG548
4UDD site 1	MET560, LEU563, ASN564, GLN570, ARG611, TYR735, THR739, ILE747,
4UDD site 2	GLU540, GLN570, TRP610, ARG611, ARG614, GLN615
4UDD site 3	ASN619, TYR640, LYS644, HIS645, TYR648, GLU727, GLU730

3. Results and discussion

3.1. Chemistry

In the present study a series of diosgenyl derivatives, including ten amino acid diosgenyl esters (**2a**–**8a** and **11a**–**14a**), two dipeptide derivatives (**9a** and **10a**), two esters of caffeic and levulinic acid (**16a** and **15**) have been synthesized.

The amino acid derivatives **2**–**8** and **11**–**14** were prepared by the esterification reaction involving *N*,*N'*–dicyclohexylocarbodiimide (DCC) and 4–dimethylaminopyridine (DMAP), corresponding *N*–*t*–butoxycarbonyl amino acids, and diosgenin in dry dichloromethane at room temperature. After the reaction had been completed, the post–reaction mixture was filtered and water was added to the residue. The organic layer was separated and washed successively with $NaHCO_{3\ aq.}$ solution, then $NaCl_{\ aq.}$ solution. The extract was dried over anhydrous $MgSO_4$, filtered and evaporated to dryness. Products **2**–**8** and **11**–**14** were then purified by flash chromatography (ethyl acetate/hexane mixture). The yield of **2**–**8** and **11**–**14** intermediates ranged from 78 to 98%. In the next step Boc groups were removed by 2.9M HCl gas in ethyl acetate. The deprotection gave appropriate hydrochlorides **2a**–**8a** and **11a**–**14a** as final products with good yields.

Dipeptide derivatives **9** and **10** were synthesized using a "step by step" method. (25*R*)–spirost–5–en–3β–yl *L*–valinate hydrochloride (**2a**) was coupled with Boc–*L*–Leu using TBTU as the coupling activator in the presence of HOBt and DIPEA in DCM [33]. Likewise, (25*R*)–spirost–5–en–3β–yl *N*–(*t*–butoxycarbonyl)–*L*–prolinate was coupled with Boc–*L*–Ile by the TBTU method in DCM. Crude products **9** and **10** were then separated by extraction and purified by flash chromatography (ethyl acetate–hexane mixture). The pure fraction was evaporated, allowing to obtain **9** and **10**. The yields were 97% and 94%, respectively. Then, Boc removal with hydrogen chloride in ethyl acetate gave hydrochlorides **9a** and **10a**.

Tigogenin derivatives **2c** and **4c** with a single bond in the C5–C6 position were obtained in the course of reducing the *N*–protected compounds **2** and **4**, with a simultaneous removal of the benzyl groups. The reduction was carried out under hydrogenation conditions with Pd/C as a catalyst in ethyl acetate. After the reaction had been completed, the mixture was filtered through a cellite pad, the filtrate was evaporated and products **2b** and **4b** were obtained with good yields. In the next step Boc groups were removed by hydrogen chloride in ethyl acetate to give hydrochlorides **2c** and **4c** with the yields of 65% and 70%.

A diosgenin derivative with caffeic acid **16** was obtained as a result of the condensation reaction of the allyl caffeic acid derivative with diosgenin (DCC, DMAP, THF) with the subsequent removal of the allyl groups (All) by 1,3–dimethylbarbituric acid in the presence of triphenylphosphine and palladium(II) acetate at 75°C. After the reaction had been completed, the mixture was filtered through a cellite pad and the filtrate was evaporated. The crude product was then separated by extraction and purified by flash chromatography with a mixture of dichloromethane and methanol to give product **16a** (yield 98%).

Levulinic acid diosgenyl ester **15** was obtained analogously as **16**, i.e. as a result of the esterification involving DCC, DMAP, levulinic acid and diosgenin in dry tetrahydrofuran at room temperature. The crude product was isolated by extraction and then purified by flash chromatography with a mixture of ethyl acetate and hexane to obtain **15** with the 60% yield.

Compound **17** was obtained by the acetylation of diosgenin with acetic anhydride in the presence of DMAP and triethylamine in dichloromethane at room temperature. The spectral data of acetate **17** was as reported earlier [34]. The F–ring of the spiroketal bond was opened under mild reductive cleavage conditions using sodium cyanoborohydride in acetic acid at room temperature [35]. As a result of the extraction and purification by flash chromatography we obtained product **18** with a good yield (98%).

Structures of all diosgenin analogues have been confirmed by spectral techniques.

3.1.1 NMR

Taking into account predictable differences in the structures of compounds **4**/**4b** and **17**/**18,** we performed a detailed ^{1}H and ^{13}C NMR comparative analysis for these pairs of analogues.

Although hydrogenation of the C5–C6 bond in **4** can theoretically lead to two different enantiomeric products originating from the attack of hydrogen on the C5 carbon from both sides of the molecule, the known examples of the diosgenin double bound hydrogenations indicated the stereoselectivity of the process [36]. In order to confirm that the spatial position of the methyl group at C10 (CH_3–19) limits the substitution of hydrogen from the above, we studied the hydrogenation product of **4**. Similarly to literature data, we isolated one product which was identified as **4b** tigogenin derivative with H3 and H5 protons in the *cis*–axial positions and the methyl group at C10 in the *trans*–axial position to proton H5. This fact was fully confirmed by the NOE effect observed in the 2D NOESY experiment where the cross–peak at δ = 4.74/1.15 ppm corresponding to H3/H5 protons was evident. Further meaningful effects proving the H3/H5 *cis* relation were noticed for the following cross–peaks: δ = 0.65/1.15 ppm (H9/H5), δ = 0.65/1.00 (H9/one of H1 protons), δ = 4.74/1.57 ppm (H3/one of H4 protons), δ = 4.74/1.80 (H3/one of H2 protons) and δ = 4.74/1.00 (H3/one of H1 protons). The formation of tigogenin derivative **4b** from diosgenin **4** was strongly related to a few significant effects reflected in the changes of the $^{1}H/^{13}C$ NMR chemical shifts. First of all, the change of a C5–C6 double bond to a single one caused significant alternations of ^{13}C NMR, as well as ^{1}H NMR chemical shifts. For C5 and C6 nuclei a shielding increase of *ca*. 95.0 ppm was recorded. Other differences were observed for C4, C8, C9, C10 and C19 nuclei. In all these cases medium shielding effects: 4.0 ppm (C4), 1.0 ppm (C10), 7.0 ppm (CH_3–19) and deshielding effects: 3.5 ppm (C8) and 4.3 ppm (C9) were calculated. The hydrogenation of the C5–C6 double bond was also related to considerable changes of the ^{1}H NMR chemical shifts but this time only shielding effects were noticed. The biggest one was observed for H6 proton (*ca*. 4.1 ppm), whereas smaller ones were for both H4 (*ca*. 0.7 – 1.0 ppm), both H7 protons (*ca*. 0.4 – 0.7 ppm), H8 (*ca*. 0.1 ppm), H9 (*ca*. 0.3 ppm) and protons of the methyl group at C10 (CH_3–19) (*ca*. 0.2 ppm).

The opening of the diosgenin ring F led to several changes of the $^{1}H/^{13}C$ NMR chemical shifts related to this structural modification. A relatively strong ^{13}C shielding increase by *ca.* 19.0 ppm was observed only in the case of C22 nucleus, whereas for other carbon nuclei in the ring opening area the opposite effects of ^{13}C shielding were noticed: C16 (*ca*. 2.5 ppm), C17 (*ca*. 3.0 ppm), CH_3–19 (*ca*. 4.4 ppm), C27 (*ca*. 1.2 ppm) and C25 (*ca*. 5.5 ppm). For the respective protons these changes were smaller and less consistent.

3.2.Biological studies

3.2.1. Anticancer activity

All synthesized compounds have been screened for their cytotoxic activity against human cancer cell lines, i.e. breast (MCF–7 and MDA–MB–231), and prostate (PC–3). Normal human umbilical vein endothelial cells (HUVEC) have also been used. The cytotoxicity was measured with an MTT assay and the cells treated with ethanol (1%) served as control (100% viability).

Table 3. The IC_{50} values (μM) of the compounds after a 48 hours incubation with the cells. Mean values with standard deviations are shown.

Compound	MCF–7[a]	PC–3[a]	MDA–MB–231[a]	HUVEC
TGG	> 100	> 100	> 100	—
1 (**DSG**)	21.0 ± 3.6	10.0 ± 2.9	20.0 ± 3.9	10.0 ± 2.5

2c	1.4 ± 1.3	10.0 ± 2.3	10.5 ± 4.3	4.5 ± 1.7
3a	8.5 ± 2.6	10.0 ± 3.3	17.0 ± 3.5	7.0 ± 2.2
4c	70.0 ± 7.4	> 100	> 100	> 100
5a	8.5 ± 2.5	16.0 ± 2.7	30.0 ± 3.6	10.5 ± 3.8
6a	7.5 ± 3.6	12.0 ± 2.4	10.5 ± 2.7	9.5 ± 2.7
7a	5.0 ± 2.3	11.0 ± 2.3	11.0 ± 3.4	5.0 ± 1.9
8a	7.5 ± 2.9	20.0 ± 5.6	11.0 ± 4.1	10.0 ± 3.6
9a	3.4 ± 2.9	7.5 ± 2.1	6.0 ± 2.0	3.0 ± 2.1
2a	8.5 ± 2.4	9.2 ± 3.0	13.0 ± 3.3	8.5 ± 2.4
10a	4.0 ± 2.7	7.5 ± 3.8	8.5 ± 3.0	3.7 ± 2.7
18	50.0 ± 2.8	60.0 ± 4.8	71.0 ± 6.2	60.0 ± 7.0
15	41.0 ± 4.4	100.0 ± 3.8	97.0 ± 5.0	51.0 ± 3.1
16a[b]	—	—	—	—
11a	7.5 ± 4.0	19.0 ± 2.5	23.0 ± 5.2	8.5 ± 1.6
12a	22.0 ± 3.4	> 100	> 100	11.0 ± 3.3
13a	7.5 ± 4.5	15.0 ± 3.9	17.0 ± 3.7	7.0 ± 3.2
14a	5.4 ± 3.7	10.0 ± 1.9	13.0 ± 3.5	7.5 ± 2.2

[a]MCF–7: mammary gland carcinoma; MDA–MB–231: breast cancer; PC–3: prostate cancer
[b]result cannot be interpreted — compound interferes with the component of the MTT test

The results of the studies on the cytotoxicity of diosgenyl derivatives are summarized in Table 3. Diosgenin and tigogenin were used as reference compounds. Most of the obtained derivatives display a cytotoxic activity higher or comparable to that of diosgenin (IC_{50}: 10 – 21μM). Interestingly, tigogenin (TGG) did not show any toxicity in the tested concentration range towards the cancer cells.

Derivative **2c** (*L*–serine in position 3 of TGG) shows the highest activity towards MCF–7 cells (IC_{50}: 1.4 μM), while its activity towards PC–3 and MDA–MB–231 cells is lower and the IC_{50} value equals 10 and 10.5 μM, respectively. Furthermore, compounds **7a** and **14a** (*L*–histidine and *L*–proline in position 3 of DSG) are also active in the tested cell line systems with the highest activity against the MCF–7 cell line. The IC_{50} value towards MCF–7 for the derivatives containing the above mentioned amino acids is 5 μM (for the reference compound 21 μM). The activity towards the PC–3 and MDA–MB–231 cells is lower and the IC_{50} value is within the range of 10 to 13 μM. Dipeptide diosgenin derivatives **9a** and **10a** have also been characterized by a high cytotoxic activity towards MCF–7 cancer cells, i.e. 3.4 μM and 4 μM, respectively, while their activity towards the PC–3 and MDA–MB–231 cells is also lower (IC_{50} from 6 to 8.5 μM). On the other hand, in the MCF–7 the IC_{50} values for derivatives **3a**, **5a**, **6a**, **8a**, **2a**, **11a**, **13a** containing amino acids (*L*–isoleucine, glycine, *L*–valine, *L*–methionine, *O*–benzyl–*L*–serine, *L*–alanine and *L*–leucine) in position 3 of DSG are by 7 μM to 8.5 μM lower than the IC_{50} values for two remaining cancer cell lines. Compounds **4c**, **12a** and **15** substituted with *L*–glutamine, *L*–phenylalanine or the levulinic acid display a low cytotoxic activity towards cancer cells.

The tested derivatives display a high antiproliferative activity towards cancer cells. The IC_{50} values show that the MCF–7 breast cancer cells are slightly more sensitive to the studied compounds than the MDA–MB–231 and PC–3 cells. At the same time, these compounds show a similar or slightly higher

cytotoxicity towards normal cells (HUVEC). An initial biological study has proved that the type of a substituent in position 3 of the DSG and TGG derivatives significantly affects their activity *in vitro*. The compounds containing amino acids such as: *L*–serine, *L*–histidine and *L*–proline as well as dipeptides (–*L*–leucyl–*L*–valine and –*L*–isoleucyl–*L*–proline) have proved to be the most active.

3.2.2. Activation of apoptosis in MCF–7 cells

Caspases are a family of endoproteases that provide critical links in cell regulatory networks controlling inflammation and cell death. Caspases involved in the apoptosis have been subclassified by their mechanism of action and are either initiator caspases (caspase–8 and –9) or executioner caspases (caspase–3, –6, and –7) [37]. Caspase–3 and caspase–7 (caspase 3/7) are strongly activated during the apoptosis, irrespective of the specific death–initiating stimulus, and coordinate the demolition phase of the apoptosis by cleaving a diverse array of protein substrates [38]. Thus, caspases 3/7 serve as markers of the apoptosis.

It has been shown previously that in some cancer cells diosgenin and its analogues activate caspases leading to apoptosis [39]. Having demonstrated that derivative **2c** (*L*–serine in position 3 of TGG) is highly toxic towards breast cancer cells (especially MCF–7) we examined its proapoptotic activity. MCF–7 cells were incubated with **2c** for 18 hours and subsequently the activity of caspases 3 and 7 was measured. Staurosporine which inhibits tumor cell growth by inducing cell death via intrinsic apoptotic pathways [40] was used as the positive control.

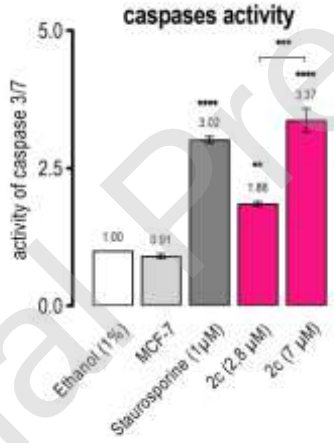

Figure 2. Activity of caspase 3/7 in MCF–7 cells treated with the test compound **2c** (2,8 µM and 7 µM) or staurosporine for 18 hours. The apoptosis was determined by the Apo–ONE® Homogeneous Caspase–3/7 Assay (Promega, Madison, WI, USA). Abbreviations: MCF–7 — untreated cells; Ethanol — MCF–7 cells treated with 1% ethanol. The caspase activation level in the cells exposed to 1% ethanol was normalized to 1.0. Means ± SD are shown. ANOVA, *post hoc* Tuckey: *p < 0.05, **p < 0.01, ***p < 0.001, ****p<0.0001 vs. Ethanol (1%).

Data presented in Figure 2 clearly demonstrate that derivative **2c** induces apoptosis in MCF–7 cells in a dose–dependent manner. The incubation of MCF–7 cells with **2c** at 2.8 µM ($2\times IC_{50}$) and 7 µM ($5\times IC_{50}$) led to 1.86–fold and 3.37–fold increase in the activity of caspase 3/7, respectively.

These results suggest that the cytotoxic activity of compound **2c** towards MCF–7 cancer cells is likely due to the induction of apoptosis.

3.2.3. Immunomodulatory activity

Six compounds have been selected for the study of their immunomodulatory properties. They differed in the steroid aglycon part (DSG, TGG) and in the substituents in position 3 of the steroid skeleton. Their immunomodulatory properties have been determined by examining the effect on the expression of several cytokine genes (IL–1, IL–4, IL–10, IL–12, TNF–α) essential for the correct functioning of the human immune system.

The studies have been performed by real time RT–PCR to measure the relative mRNAs levels in the THP–1 cells after a 6 hours incubation with LPS (5 μg/ml) or the tested compounds (5 μM). Under these experimental conditions the viability of the THP–1 cells has exceeded 90% (data not shown). Levels of the analyzed mRNAs in THP–1 cells treated with 1% ethanol have been used as control (K). LPS (a strong activator of the cytokine expression and secretion) has been used as the reference compound (positive control).

Out of five tested cytokines, three: IL–1, TNF–α and IL–12 have a pro–inflammatory activity, while IL–10 is an anti–inflammatory cytokine. Depending on the biological context, IL–4 can have either a pro– or anti–inflammatory effect.

Pro–inflammatory IL–1, TNF–α and IL–12 are the mediators in various acute and chronic inflammation linked diseases [41]. The immunomodulatory IL–10 plays a crucial role in the maintenance of homeostasis, particularly in controlling immunopathology of infectious, allergic and autoimmune diseases [42]. IL–4 is a cytokine that regulates multiple biological functions. It can regulate proliferation, apoptosis and plays a critical role in the regulation of immune responses [43].

The results shown in Figure 3 reveal that the effect of compounds **2c**, **4c**, **9a**, **15**, **16a**, **18** on the expression of pro–inflammatory IL–1 is similar to that of diosgenin. Interestingly, analogues **4c** and **16a** show a statistically significant inhibition of the expression of TNF–α when compared to diosgenin. On the other hand, **9a** stimulates the expression of TNF–α with a statistical significance vs. K. Comparison of TGG and **4c** (a tigogenin derivative) reveals that both compounds have a similar effect on the expression of the TNF–α, IL–1 and IL–12 genes in the THP–1 cells.

We have also evaluated the effect of the synthesized diosgenin and tigogenin analogues on the expression of anti–inflammatory IL–10. Our studies indicate that analogues **4c**, **9a**, **16a** cause a significant induction of the IL–10 expression. This effect is statistically significant vs. both K (untreated cells) and diosgenin or tigogenin treated cells. Most of the tested compounds also strongly upregulates the expression of IL–4 in comparison to the untreated cells (K), except for **2c** and **9a** which do not have a significant effect on the expression of this cytokine.

From among diosgenin analogues tested, compounds **4c** and **16a** exhibit the desired immunomodulatory effects. They do not induce the expression of pro–inflammatory cytokines, while stimulating the expression of anti–inflammatory IL–10 in the THP–1 monocytes. Moreover, their immunomodulatory activity is higher than that of diosgenin or tigogenin.

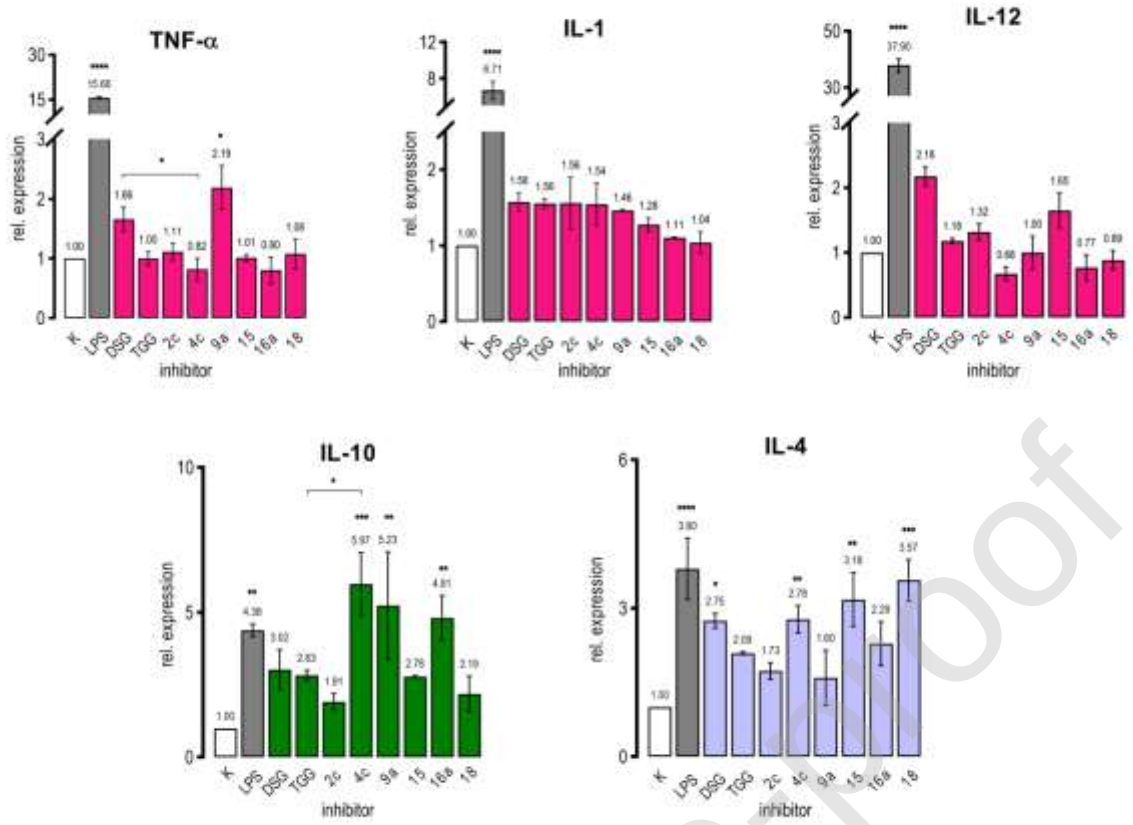

Figure 3. Relative expression of the cytokine genes in the THP–1 cells after incubation with the tested compounds in relation to control (K). Means ± SD are shown. ANOVA, *post hoc* Tuckey: *p < 0.05, **p < 0.01, ***p < 0.001, ****p<0.0001 vs. Ethanol (1%).

3.4. Computational methods

Table 4.Predicted ADMET properties calculated for the tested compounds

Compd	MW[a]	Dipole[b]	Volume[c]	SASA[d]	donorHB[e]	accptHB[f]	logP[g]	#metab[h]	P[i]	Ro5[j]	Ro3[k]
TGG	416.6	2.05	1324.16	681.95	1.00	3.20	6.01	1	4180	1	1
DSG 1	414.63	1.94	1317.60	685.17	1.00	3.20	6.00	3	4172	1	1
2a	591.83	5.75	1956.67	11077.78	1.00	6.70	8.73	5	3414	2	1
2c	501.71	6.43	1620.07	893.33	1.00	5.70	6.41	4	1116	2	1
3a	527.79	5.43	1749.95	954.16	1.00	5.00	7.94	3	3826	2	1
4c	543.74	7.68	1739.09	955.76	2.00	7.00	6.52	4	73	2	1
5a	471.68	6.03	1547.09	858.38	1.00	5.00	6.36	3	1605	1	1
6a	513.76	5.54	1699.41	929.95	1.00	5.00	7.61	3	3826	2	1
7a	551.77	11.26	1766.49	966.60	2.00	7.00	6.58	4	764	2	1
8a	545.82	7.30	1785.13	983.09	1.00	5.50	8.01	3	3038	2	1
9a	626.92	7.56	1847.83	920.80	2.25	6.25	6.03	5	63	2	1

10a	624.90	11.35	1922.44	1006.99	2.00	8.50	6.06	6	631	2	1
11a	485.71	5.72	1602.34	885.47	1.00	5.00	6.86	3	2517	1	1
12a	561.80	5.82	1820.29	993.01	1.00	5.00	8.58	4	3727	2	1
13a	527.79	5.88	1740.23	938.66	1.00	5.00	7.83	3	3323	2	1
14a	511.74	6.23	1541.81	782.77	1.00	5.00	6.56	4	3274	2	1
15	512.73	2.71	1602.20	829.08	0.00	5.50	6.46	4	1297	2	1
16a	576.77	3.99	1794.87	932.28	2.00	5.00	7.54	4	2548	2	1
18	456.66	6.37	1412.44	728.03	0.00	3.50	6.41	2	462	1	1

[a]MW – molecular weight (Da); [b]dipole – dipole moment (D); [c]volume – total molecular volume (Å^3); [d]SASA – solvent accessible surface (Å^2); [e]donorHB – estimated number of hydrogen bonds that would be donated by the solute to water molecules in an aqueous solution; [f]accptHB – estimated number of hydrogen bonds that would be accepted by the solute from water molecules in an aqueous solution; [g]logP – octanol/water partition coefficient; [h]#metab – number of likely metabolic reactions; [i]P – apparent Caco–2 permeability (nm/sec); [j]Ro5 – number of violations of Lipinski's rule of five; [k]Ro3 – number of violations of Jorgensen's rule of three.

Ten predicted ADME properties have been calculated for all analyzed compounds. Principal descriptors are given in Table 4. Lipinski's rule describing the essential physicochemical characteristics of well–known medicines with good oral bioavailability determines that the mass of a potential drug substance should not exceed 500 Da [44]. Molecular weights of the tested molecules fall within the range 414.627 – 626.918 which constitutes the limits currently suggested for multi–target drugs (130.0 – 725.0). For all compounds the computed dipole moment and the total solvent–accessible volume values are within the limits traditionally prescribed for those parameters. Total solvent accessible surface area (SASA) values have been predicted as 1077.783 Å^2 for **2a** and 1006.987 Å^2 for **10a**, exceeding the traditionally cutoff value of 1000.000, but only to a small extent. For other compounds they fall within the limit of 300.0 – 1000. The estimated number of hydrogen bonds that would be donated by the solute to the water molecules in an aqueous solution (donorHB) and the estimated number of hydrogen bonds that would be accepted by the solute from the water molecules (accptHB), same as the number of likely metabolic reactions (#metab), are in accordance with Lipinski's rule. The logP values fall within the range 6.000 – 8.729 for the majority of compounds, which is not in an agreement with the values for the well absorbed compounds (recommended values for log P are –2.0 – 6.5), and indicates even higher lipophilicities.

The aim of the ADME screening was to eliminate poor lead candidates from the family of diosgenin and tigogenin derivatives at this early stage of our studies. It has bee demonstrated that the compounds tested did not meet the requirements of one (**TGG**, **DSG**, **5a**, **11a**, **18**) or two (**2a**, **2c**, **3a**, **4c**, **6a**–**10a**, **12a**–**14a**, **15**) requirements of Lipinski's rule of five and one requirement of Jorgensen's rule of three (taking into account aqueous solubility of the compound, Caco–2 cell permeability and number of primary metabolites). These values indicate the number of potential ADME risk factors that the compounds might possess in terms of their suitability for an orally active drug. There is, however, a number of drugs that fall outside of Lipinski's rule of five, particularly among the natural products and their derivatives. In some cases, they do not meet the molecular weight and number of hydrogen bond acceptors criteria [45]. In view of these findings the ADME profile for our diosgenin and tigogenin derivatives shows that they constitute a promising scaffold for further modification of more potent and selective agents.

3.5. Molecular interaction study of DSG and TGG analogues through docking

The aim of the molecular interaction study has been to explore the molecular interaction of the DSG and TGG analogues with the estrogen receptor (ER) and glucocorticoid receptor (GR). The estrogen receptor is an important therapeutic target in the clinical treatment of breast cancer [46], while the GR is expressed in almost every cell in the body and regulates genes that control, *inter alia*, the immune response [47]. Assuming that the structures of diosgenin and tigogenin are similar to that of glucocorticoids (GCs) which bind to the GR and are important chemicals widely used in the therapy of inflammatory diseases, we have hypothesized that **4c** and **16a** might function by affecting the GRs involved in the anti–inflammatory pathways.

*3.5.1. Molecular docking of **2c** to the estrogen receptor*

Molecular docking of **2c** to three different potential binding sites of the estrogen receptor has revealed that two of these sites show relatively low affinities (low nM for site 3 and high nM for site 2) with respect to site 1 (K_i = 3.73 pm) which was the binding site of the co–crystalized estradiol derived metal chelate. We can see that the predicted binding pose of **2c** is very similar to the binding pose of the estradiol derivative, since both ligands occupy the same space and interact with the same residues, apart from HIS524. **2c** is particularly predicted to make two strong hydrogen bonds between the terminal –OH group and GLU353/ARG394, just like the estradiol derivative from the crystal structure. The obtained affinity value of K_i = 3.73 pM (Table 5) pm is better than the values obtained for **1** (K_i = 39.65 pm) and TGG (K_i = 26.30 pm) suggesting a more suitable fit to the binding site of the estrogen receptor than for these two natural compounds, though the binding pose is very similar in all three cases. Indeed, while the predicted binding pose of all three compounds is comparable, either **1** or TGG can only make one hydrogen bond to GLU353 which stabilizes these systems in the binding site, but to a lesser degree than **2c**. For the sake of comparison we have also performed molecular docking of diethylstilbestrol, a known nonsteroidal estrogen receptor agonist used in the past for a variety of medical conditions [48]. The obtained pose was virtually identical with the diethylstilbestrol pose from the crystal structure of its complex with the estrogen receptor [49], with one of the hydroxyl groups interacting with both GLU353 and ARG394. The estimated K_i for this pose is 26.88 nM, which is four orders of magnitude worse than for **2c**.

Table 5. Estimated computational Ki values from the molecular docking.

compound	estrogen receptor K_i	glucocorticoid receptor K_i
TGG	26.30 pM	9.17 pM
1	39.65 pM	11.89 pM
2c	3.73 pM	—
4c	—	0.23 pM
16a	—	1.14 pM
diethylstilbestrol	26.88 nM	—
mifepristone	—	17.15 pM

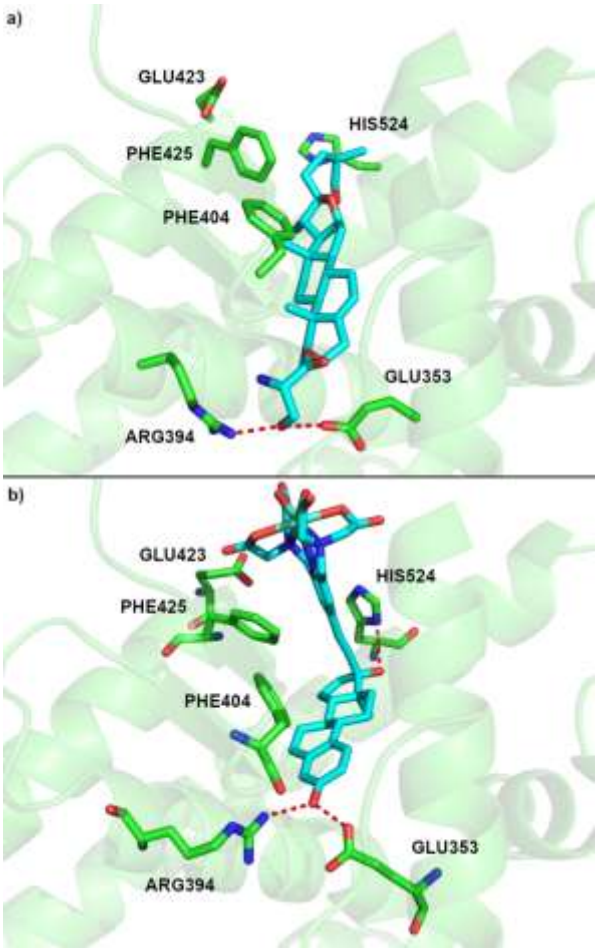

Figure 4. Comparison of the **a)** calculated pose of **2c** and **b)** crystal structure pose of the estradiol derivative in the estrogen receptor binding site.

*3.5.2. Molecular docking of **4c** and **16a** to the glucocorticoid receptor*

Molecular docking of **4c** and **16a** to three different potential binding sites of the GR has revealed that all three sites show relatively high free energies of binding and the K_i values in the low nM range. Site 3, located at the outer surface of the GR is, however, an unlikely candidate for a binding site. We have therefore focused our attention on the first two sites. All four best found poses of **4c** and **16a** in these two sites are stabilized mostly by hydrophobic/van der Waals interactions with a small number of hydrogen bonds. The best pose of **16a** is stabilized in the binding pocket (corresponding to the binding pocket of the desisobutyrylciclesonide from the complex crystal structure) by three hydrogen bonds to ASN564, ARG611 and THR739 with the binding affinity of 1.14 pM (Table 5). Interestingly, **4c** in the same binding site also displays a low K_i of 5.6 pM and a very similar pose stabilized by hydrogen bonds to ARG611 and THR739 as well as to GLN570. The poses of **4c** and **16a** in the second site are, on the other hand, quite different. Here, **16a** with the binding affinity of 1.8 pM is also stabilized by a hydrogen bond to ARG611 and partially occupies the binding pocket of desisobutyrylciclesonide, while **4c** is shifted away from site 1 and is in different orientation than **16a**, stabilized by a hydrogen bond to ARG614 (binding affinity of 0.2 pM). **1** and **TGG** are predicted to bind preferentially to site 1 with lower binding affinities than both **4c** and **16a** (K_i = 9.68 pM in the case **1** and K_i = 11.88 for **TGG**). It is interesting to note, however, that **TGG** is predicted to bind in a pose similar to **4c** with the lone hydroxyl group pointing towards ARG611, while in the case of **1** the hydroxyl group is pointing towards TYR735. In this case we also decided to compare these results with the binding affinity of a known drug

interacting with the glucocorticoid receptor. We have selected mifepristone which is used for medical abortion [50]. In molecular docking we were able to find mifepristone pose very similar to the one from the crystal structure [51] with the estimated binding affinity of 521.9 pM, two–three orders of magnitude worse than for **4c** and **16a**.

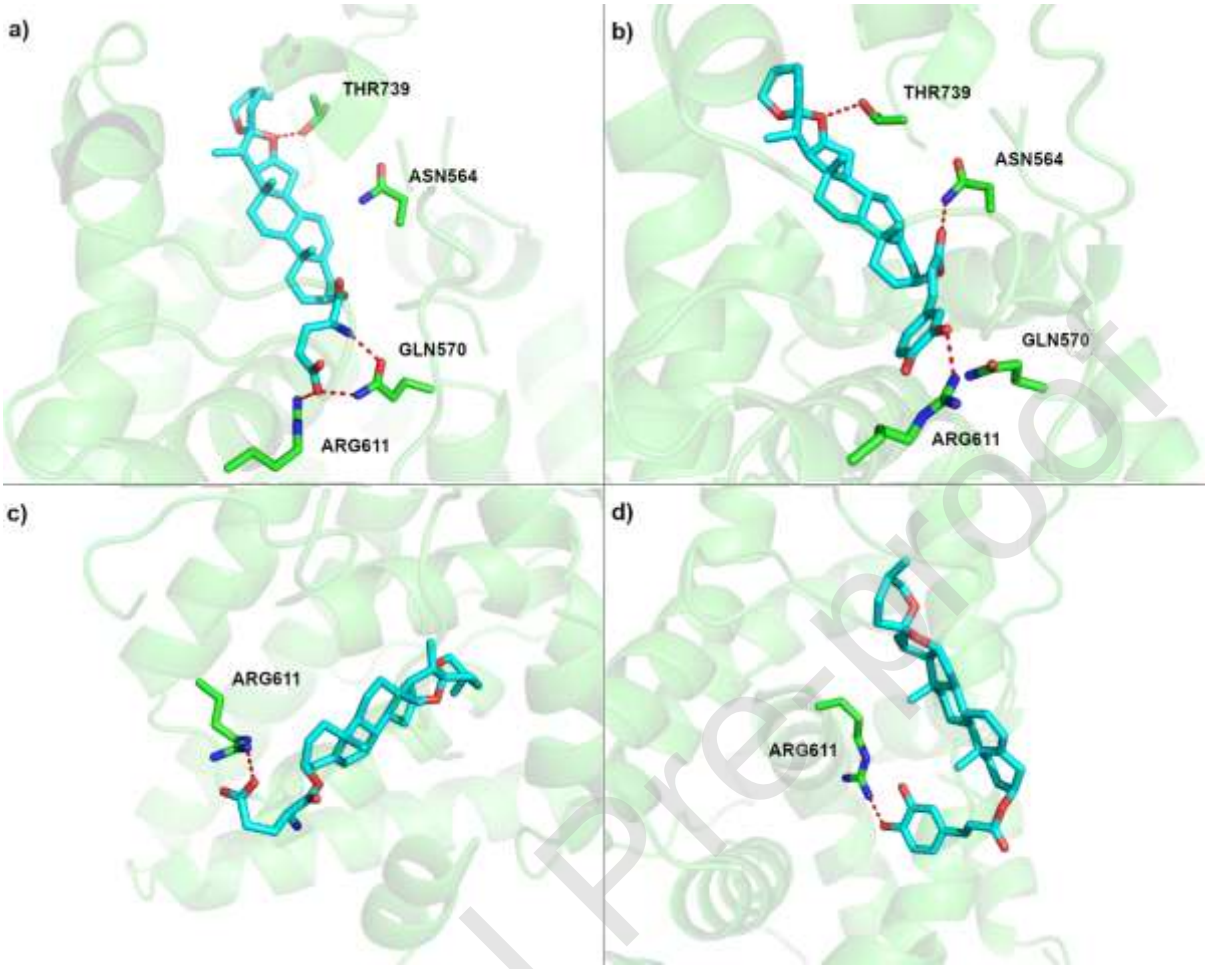

Figure 5. Comparison of the calculated pose of **a) 4c** and **b) 16a** (both in site 1) and **c) 4c** and **d) 16a** (site 2) in the GR binding site.

The obtained affinity values for all investigated compounds (in the fM–pM range) seem unrealistically high, but given the expected accuracy of the docking algorithm of around 1–2 kcal/mol we can expect affinities in the low nM values for all the tested systems. Unfortunately, while the protocol used in this investigation is generally accurate in predicting ligand poses within the binding sites of receptors, it may be often inaccurate when it comes to estimating binding free energies; it has been shown that the latter values may err by a few orders of magnitude [52,53]. Therefore, we should treat high computational affinity values only as indicators of possible high–affinity compounds, but such results need to be later confirmed by experimental estimates. At the same time, with relatively high confidence we can treat the obtained ligand poses as accurate.

4. Conclusion

In conclusion, we have synthesized a set of diosgenin and tigogenin derivatives substituted with various amino acids, a dipeptide or levulinic and 3,4–dihydroxycinnamic acid at C–3 position that have been further evaluated for their antiproliferative and anti–inflammatory activity. Diosgenin and tigogenin analogues display a high antiproliferative activity towards breast (MCF–7 and MDA–MB–

231) and prostate (PC–3) human cancer cell. The serine derivative of tigogenin **2c** shows the highest cytotoxic activity towards MCF–7 cells and induces apoptosis. Possible mechanism of the antiproliferative action of compound **2c** is through the caspase dependent apoptosis pathway.

Diosgenin and tigogenin conjugates also show immunomodulatory properties. Structure–activity relationship studies indicate that compounds **4c** and **16a** in most cases exhibit desired effects. They do not induce the gene expression of the pro–inflammatory cytokines (i.e. IL–12, IL–1, TNF–α) but strongly stimulate the expression of anti–inflammatory IL–10 and IL–4.

Ten predicted ADME properties have been calculated for all the obtained compounds. The compounds tested have not met the requirements of one (**1**, **5a**, **11a**, **18**) or two (**2a**, **2c**, **3a**, **4c**, **6a**–**10a**, **12a**–**14a**, **15**) regulations of Lipinski's rule of five and one requirement of Jorgensen's rule of three (taking into account only such parameters as molecular weight and the number of hydrogen bond donors and acceptors). The synthesized compounds exhibit reasonable ADME properties, which may be an indication of their good oral drug–like behavior.

A molecular docking study has revealed a high binding affinity of diosgenin and tigogenin analogues to the active site of the glucocorticoid receptor (GR) and the estrogen receptor (ER). Our findings have shown that analogue **2c** interacts with amino acids GLU353/ARG394 at the binding site of ER with inhibition constant K_i = 3.73 pM, This value is four orders of magnitude better than for reference diethylstilbestrol. Compounds **4c** and **16a** also revealed strong binding interaction with the active site GR with the inhibition constant K_i = 0.23 pM and K_i = 1.14 pM respectively. The estimated binding affinity (K_i) of **4c** and **16a** is two–three orders of magnitude better than for the known drug mifepristone. The molecular docking results indicated that **2c**, **4c** and **16a** derivatives exhibited a higher affinity for the ER and the GR active site than the known drug.

Promising *in vivo* anti–tumor and immunomodulating activity, molecular docking, and drug–likeness properties of compounds **2c**, **4c**, **16a** indicate that these compounds can serve as potential lead compounds for further development and investigation of novel anticancer and immunomodulatory agents.

Conflict of interest

There is no conflict of interest.

Acknowledgements

This work was supported under the framework of the statutory project funded by the Polish Ministry of Science and Higher Education.

References

[1]a) L. Fernández–Cabezón, B. Galán, J.L. García New Insights on Steroid Biotechnology, Front. Microbiol. 9 (2018) 958. https://doi.org/10.3389/fmicb.2018.00958. b) A. Parus, Postępy Fitoterapii, Pharmacological activities of saponins, 3 (2013) 200–204.
[2] G. Gu, L. An, M. Fang, Z. Guo, Efficient one–pot synthesis of tigogenin saponins and their antitumor activities, Carbohydr. Res. 383 (2014) 21–26. https://doi.org/10.1016/j.carres.2013.10.015.

[3] a) Z. Wang , Y. Cheng , N. Wang , D. M. Wang , Y. W. Li , F. Han , J. G. Shen , D. P. Yang , X. Y. Guan, J. P. Chen, Dioscin induces cancer cell apoptosis through elevated oxidative stress mediated by downregulation of peroxiredoxins, Cancer Biol. Ther. 13 (2012) 138–147. https://doi.org/10.4161/cbt.13.3.18693. b) K. Patel, M. Gadewar, V. Tahilyani, D. K. Patel, A review on pharmacological and analytical aspects of diosgenin: a concise report, Nat. Prod. Bioprospect. 2 (2012) 46–52. https://doi.org/10.1007/s13659–012–0014–3. c) J. Raju, R. Mehta, Cancer chemopreventive and therapeutic effects of diosgenin, a food saponin, Nutr. Cancer 61 (2009) 27–35. https://doi.org/10.1080/01635580802357352.
[4] F. Wang, J. Tang, Z. Wu, Flora of China; Science Press, 1980.
[5] C. Corbiere, B. Liagre, A. Bianchi, K. Bordji, M. Dauca, P. Netter, J. L. Beneytout, Different contribution of apoptosis to the antiproliferative effects of diosgenin and other plant steroids, hecogenin and tigogenin, on human 1547 osteosarcoma cells, Int. J. Oncol. 22 (2003) 899–905. https://doi.org/10.3892/ijo.22.4.899.
[6] G. L. Li, H. J. Xu, S. H. Xu, W. W. Wang, B. Y. Yu, J. Zhang, Synthesis of tigogenin MeON–Neoglycosides and their antitumor activity, Fitoterapia 125 (2018) 33–40. https://doi.org/10.1016/j.fitote.2017.12.014.
[7] a)J. Raju, J. M. Patlolla, M. V. Swamy, C. V. Rao, Diosgenin, a steroid saponin of Trigonellafoenum graecum (Fenugreek), inhibits azoxymethane–induced aberrant crypt foci formation in F344 rats and induces apoptosis in HT–29 human colon cancer cells, Cancer Epidemiol. Biomarkers Prev. 13 (2004) 1392–1398; b) V. S. Malisetty, J. M. R. Patlolla, J. Raju, L. A. Marcus, C. L. Choi, C. V. Rao, Chemoprevention of colon cancerby diosgenin, a steroidal saponin constituent of fenugreek, Proc. Am. Assoc. Cancer Res. 46 (2005) 2473; c) T. Yamada, M. Hoshino, T. Hayakawa, H. Ohhara, H. Yamada, T. Nakazawa, T. Inagaki, M. Iida, T. Ogasawara, A. Uchida, C. Hasegawa, G. Murasaki, M. Miyaji, A. Hirata, T. Takeuchi, Dietary diosgenin attenuates subacute intestinal inflammation associated with indomethacin in rats, Am. J. Physiol. 273 (2009) G355–G364. https://doi.org/10.1152/ajpgi.1997.273.2.G355.
[8] C. Lepage, B. Liagre, J. Cook–Moreau, A. Pinon, J. L. Beneytout, Cyclooxygenase–2 and 5–lipoxygenase pathways in diosgenin–induced apoptosis in HT–29 and HCT–116 colon cancer cells, Int. J. Oncol. 36 (2010) 1183–1191. https://doi.org/10.3892/ijo_00000601.
[9] J. Raju, R. P. Bird, Diosgenin, a naturally occurring furostanol saponin suppresses 3–hydroxy–3–methylglutaryl CoA reductase expression and induces apoptosis in HCT–116 human colon carcinoma cells, Cancer Lett. 255 (2007) 194–204. https://doi.org/10.1016/j.canlet.2007.04.011.
[10] Ch. T. Chiang, T .D. Way, S. J. Tsai, J. K. Lin, Diosgenin, a naturally occurring steroid, suppresses fatty acid synthase expression in HER2–overexpressing breast cancer cells through modulating Akt, mTOR and JNK phosphorylation, FEBS Lett. 581 (2007) 5735–5742. https://doi.org/10.1016/j.febslet.2007.11.021.
[11] a)S. Srinivasan, S. Koduru, R. Kumar, G. Venguswamy, N. Kyprianou, C. Damodaran, Diosgenin targets Akt-mediated prosurvival signaling in human breast cancer cells, Int. J. Cancer 125 (2009) 961–967. https://doi.org/10.1002/ijc.24419. b)S. Sowmyalakshmi, R. Ranga, C.G Gairola, D. Chendil, Effect of diosgenin (Fenugreek) on breast cancer cells. Proc. Am. Assoc. Cancer Res. 46 (2005) 1382.
[12] P. S. Chen, Y. W. Shih, H. Ch. Huang, H. W. Cheng, Diosgenin, a steroidal saponin, inhibits migration and invasion of human prostate cancer PC–3 cells by reducing matrix metalloproteinases expression, PLoS ONE 6 (2011) e20164. https://doi.org/10.1371/journal.pone.0020164.
[13] F. Li, P. P. Fernandez, P. Rajendran, K. M. Hui, G. Sethi, Diosgenin, a steroidal saponin, inhibits STAT3 signaling pathway leading to suppression of proliferation and chemosensitization of human hepatocellular carcinoma cells, Cancer Lett. 292 (2010) 197–207. https://doi.org/10.1016/j.canlet.2009.12.003.
[14] M. J. Liu, Z. Wang, Y. Ju, R. N. S. Wong, Q. Y. Wu, Diosgenin induces cell cycle arrest and apoptosis in human leukemia K562 cells with the disruption of Ca^{2+} homeostasis, Cancer Chemother. Pharmacol. 55 (2005) 79-90. https://doi.org/10.1007/s00280-004-0849-3.
[15] a) B. Liagre, P. Vergne–Salle, C. Corbiere, J. L.Charissoux, J. L. Beneytout, Diosgenin, a plant steroid, induces apoptosis in human rheumatoid arthritis synoviocytes with cyclooxygenase–2 overexpression, Arthritis Res. Ther. 6 (2004) R373.https://doi.org/10.1186/ar1199.b) J. Stefanowicz-Hajduk, J. R. Ochocka, Steroidal saponins – occurrence, characteristic and application in therapeutics, Postępy Fitoterapii 1 (2006) 36;c) B. Liagre, P. Vergne–Salle, D. Y. Leger, J. L. Beneytout, Inhibition

of human rheumatoid arthritis synovial cell survival by hecogenin and tigogenin is associated with increased apoptosis, p38 mitogen–activated protein kinase activity and upregulation of cyclooxygenase–2, Int. J. Mol. Med. 20 (2007) 451–460.https://doi.org/10.3892/ijmm.20.4.451.
[16] J. X. Song, L. Ma, J.P. Kou, B.Y. Yu, Diosgenin reduces leukocytes adhesion and migration linked with inhibition of intercellular adhesion molecule–1 expression and NF–κB p65 activation in endothelial cells, Chin. J. Nat. Med. 10 (2012) 142–149.
https://doi.org/10.3724/SP.J.1009.2012.00142.
[17] Z. He, Y. Tian, X. Zhang, B. Bing, L. Zhang, H. Wang, W. Zhao, Anti–tumour and immunomodulating activities of diosgenin, a naturally occurring steroidal saponin, Nat. Prod. Res. 26 (2012) 2243–2246. https://doi.org/10.1080/14786419.2011.648192.
[18] M. Singh, A.A. Hamid, A. K. Maurya, O. Prakash, F. Khan, A. Kumar, O.O. Aiyelaagbe, A.S. Negi, D.U. Bawankule, J. Steroid Biochem. 143 (2014) 323–333.
https://doi.org/10.1016/j.jsbmb.2014.04.006
[19] L. L. Romero–Hernández, P. Merino–Montiel, S. Montiel–Smith, S. Meza–Reyes, J. L.Vega–Báez, I. Abasolo, S. Jr. Schwartz, Ó. López, J. G. Fernández–Bolaños, Diosgenin–based thio(seleno)ureas and triazolyl glycoconjugates as hybrid drugs. Antioxidant and antiproliferative profile, Eur. J. Med. Chem. 99 (2015) 67– 81. https://doi.org/10.1016/j.ejmech.2015.05.018.
[20] M. Kvasnica, M. Budesinsky, J. Swaczynova, V. Pouzar, L. Kohout, Platinum(II) complexes with steroidal esters of *L*–methionine and *L*–histidine: synthesis, characterization and cytotoxic activity, Bioorg. Med. Chem. 16 (2008) 3704–3713. https://doi.org/10.1016/j.bmc.2008.02.003.
[21] B. Huang, D. Du, R. Zhang, X. Wu, Z. Xing, Y. He, W. Huang, Synthesis, characterization and biological studies of diosgenyl analogues, Bioorg. Med. Chem. Lett. 22 (2012) 7330–7334.
https://doi.org/10.1016/j.bmcl.2012.10.086.
[22] B. Z. Huang, G. Xin, L. M. Ma, Z. L. Wei, Y. Shen, R. Zhang, H. J. Zheng, X. H. Zhang, H. Niu, W. Huang, Synthesis, characterization, and biological studies of diosgenyl analogs, J. Asian Nat. Prod. Res. 19 (2017) 272–298. https://doi.org/10.1080/10286020.2016.1202240.
[23] R. Masood Ur, Y. Mohammad, K.M. Fazili, K.A. Bhat, T. Ara, Synthesis and biological evaluation of novel 3–*O*–tethered triazoles of diosgenin as potent antiproliferative agents, Steroids 118 (2017) 1–8. https://doi.org/10.1016/j.steroids.2016.11.003.
[24] A.A. Hamid, T. Kaushal, R. Ashraf, A. Singh, A. Chand Gupta, O. Prakash, J. Sarkar, D. Chanda, D.U. Bawankule, F. Khan, K. Shanker, O.O. Aiyelaagbe, A.S. Negi, (22beta, 25*R*)–3beta–hydroxy–spirost–5–en–7–iminoxy–heptanoic acid exhibits anti–prostate cancer activity through caspase pathway, Steroids 119 (2017) 43–52. https://doi.org/10.1016/j.steroids.2017.01.001.
[25] World Cancer Report, International Agency for Research on Cancer, World Health Organization, 2014
[26] M. C. Pirrung, The Synthetic Organic Chemist's Companion; John Wiley & Sons, Inc., 2006; pp. 171–172.https://doi.org/10.1002/9780470141045.app3.
[27]a) M. Maszewska, J. Leclaire, M. Cieslak, B. Nawrot, A. Okruszek, A. M. Caminade, J. P. Majoral, Water–soluble polycationic dendrimers with a phosphoramidothioate backbone: preliminary studies of cytotoxicity and oligonucleotide/plasmid delivery in human cell culture, Oligonucleotides13 (2003) 193–205. http://doi.org/10.1089/154545703322460586. b) E. A. Jaffe, R. L. Nachman, C. G. Becker, C. R. Minick, Culture of Human Endothelial Cells Derived from Umbilical Veins. Identification by morphologic and immunologic criteria, J. Clin. Invest. 52 (1973) 2745–2756.
https://doi.org/10.1172/JCI107470.
[28] P. Boeuf., I. Vigan–Womas, D. Jublot, S. Loizon, J. C. Barale, B. D. Akanmori, O. Mercereau–Puijalon, C. Behr, CyProQuant–PCR: a real time RT–PCR techniqueforprofiling human cytokines, based on external RNA standards, readily automatable forclinicaluse, BMC Immunol. 6 (2005) 1–14.
https://doi.org/10.1186/1471–2172–6–5.
[29] C. Klein, I. Waldhauer, V. G. Nicolini, A. Freimoser–Grundschober, T. Nayak, D. J. Vugts, C. Dunn, M. Bolijn, J. Benz, M. Stihle, S. Lang, M. Roemmele, T. Hofer, E. van Puijenbroek, D. Wittig, S. Moser, O. Ast, P. Brünker, I. H. Gorr, S. Neumann, M. C. de Vera Mudry, H. Hinton, F. Crameri, J. Saro, S. Evers, C. Gerdes, M. Bacac, G. van Dongen, E. Moessner, P. Umaña, Cergutuzumabamunaleukin (CEA–IL2v), a CEA–targeted IL–2 variant-based immunocytokine forcombination cancer immunotherapy: Overcoming limitations of aldesleukin and conventional IL–2-

based immunocytokines, OncoImmunology 6 (2017) e1277306.https://doi.org/10.1080/2162402X.2016.1277306.
[30] K. Edman, A. Hosseini, M. K. Bjursell, A. Aagaard, L. Wissler, A. Gunnarsson, T. Kaminski, C. Köhler, S. Bäckström, T. J. Jensen, A. Cavallin, U. Karlsson, E. Nilsson, D. Lecina, R. Takahashi, C. Grebner, S. Geschwindner, M. Lepistö, A. C. Hogner, V. Gualla, Ligand Binding Mechanism in Steroid Receptors: From Conserved Plasticity to Differential Evolutionary Constraints, Structure 23 (2015) 2280–2290. https://doi.org/10.1016/j.str.2015.09.012.
[31] G. M. Morris, R. Huey, W. Lindstrom, M.F. Sanner, R.K. Belew, D.S. Goodsell, A.J. Olson, AutoDock4 and AutoDockTools4: Automated docking with selective receptor flexibility, J. Comput. Chem. 30 (2009) 2785–2791. https://doi.org/10.1002/jcc.21256.
[32] Z. Wang, H. Sun, X. Yao, D. Li, L. Xu, Y. Li, S. Tiand, T. Hou, Comprehensive evaluation of ten docking programs on a diverse set of protein–ligand complexes: the prediction accuracy of sampling power and scoring power, Phys. Chem. Chem. Phys. 18 (2016) 12964–12975. https://doi.org/10.1039/c6cp01555g.
[33] N. Sewald, H. Jakubke, Peptides: Chemistry and Biology, WILEY–VCH, 2002.
[34] N. Chaosuancharoen, N. Kongkathip, B. Kongkathip, A Novel Synthetic Approach from Diosgenin to a 17α–Hydroxy Orthoester via a Regio– and Stereo–Specific Rearrangement of an Epoxy Ester, Synthetic Commun. 34 (2004) 961–983. https://doi.org/10.1081/SCC-120028627.
[35] A. A. Hamid, M. Hasanain, A. Singh, B. Bhukya, Omprakash, P. G. Vasudev, J. Sarkar, D. Chanda, F. Khan, O. O. Aiyelaagbe, A. S. Negi, Synthesis of novel anticancer agents through opening of spiroacetal ring of diosgenin, Steroids 87 (2014) 108–118. https://doi.org/10.1016/j.steroids.2014.05.025
[36] a) J. R. Williams, H. Gong, N. Hoff, O. I. Olubodun, P. J. Carroll, Alpha–hydroxylation at C–15 and C–16 in cholesterol: synthesis of (25*R*)–5alpha–cholesta–3beta,15alpha,26–triol and (25*R*)–5alpha–cholesta–3beta,16alpha,26–triol from diosgenin, Org. Lett. 6 (2004) 269. https://doi.org/10.1021/ol036257u; b) Y. Li, Y. Zhang, T. Guo, H. Guan, Y. Hao, B. Yu, Synthesis of the cytotoxic Gitogenin 3b–*O*–[2–*O*–(α–*L*–Rhamnopyranosyl)–β–*D*–galactopyranoside] and its congeners 6 (2006) 775–782. https://doi.org/10.1055/s–2006–926316.
[37] D.R Mcllwain, T. Berger, T.W Mak, Caspase functions in cell death and disease, Cold Spring Harb. Perspect. Biol. 5 (2013) a008656. https://doi.org/10.1101/cshperspect.a008656
[38] J. G. Walsh, S. P. Cullen, C. Sheridan, A. U. Lüthi, Ch. Gerner, S. J. Martin, Executioner Caspase–3 and Caspase–7 Are Functionally Distinct Proteases, Proc. Natl. Acad. Sci. U S A., 105 (2008) 12815-12819. https://doi.org/10.1073/pnas.0707715105.
[39] a) D.S. Kim, B.K. Jeon, Y.E. Lee, W.H. Woo, Y.J. Mun, Diosgenin induces apoptosis in HepG cells through generation of reactive oxygen species and mitochondrial pathway, Evidence Based Compliment. Alternat. Med. (2012) 981675. https://doi.org/10.1155/2012/981675; b) S. Ghosh, P. More, A. Derle, R. Kitture, T. Kale, M. Gorain, A. Avasthi, P. Markad, G.C. Kundu, S. Kale, D.D. Dhavale, J. Bellare, B.A. Chopade, Diosgenin functionalized iron oxide nanoparticles as novel nanomaterial against breast cancer, J. Nanosci. Nanotechnol. 15 (2015) 9464–9472. https://doi.org/10.1166/jnn.2015.11704; c) L. Sanchez–Sanchez, M.G. Hernandez–Linares, M.L. Escobar, H. Lopez–Munoz, E. Zenteno, M.A. Fernandez–Herrera, G.Guerrero–Luna, A. Carrasco–Carballo, J. Sandoval–Ramirez, Antiproliferative, cytotoxic, and apoptotic activity of steroidal oximes in cervicouterine cell lines, Molecules 21 (2016) 1533. https://doi.org/10.3390/molecules21111533.
[40] A. Antonsson, J.L. Persson, Induction of apoptosis by Staurosporine involves the inhibition of expression of the major cell cycle proteins at the G2/M checkpoint accompanied by alterations in Erk and Akt kinase activities, Anticancer Res. 29 (2009) 2893–2898. http://ar.iiarjournals.org/content/29/8/2893.long
[41] I. Christiaens, D. B. Zaragoza, L. Guilbert, S. A. Robertson, B. F. Mitchell, D. M. Olson, Inflammatory processes in preterm and term parturition, J. Reprod. Immunol. 79 (2008) 50–57. https://doi.org/10.1016/j.jri.2008.04.002
[42] R. E. Mitchell, M. Hassan, B. R. Burton, G. Britton, E. V. Hill, J. Verhagen, D. C. Wraith, IL–4 enhances IL–10 production in Th1 cells: implications for Th1 and Th2 regulation, Scientific Reports 7 (2017) 11315. https://doi.org/10.1038/s41598–017–11803–y
[43] a) K. Nelms, A. D. Keegan, J. Zamorano, J. J. Ryan, W. E. Paul, The IL–4 receptor: signaling mechanisms and biologic functions, Annu. Rev. Immunol. 17 (1999) 701–738.

https://doi.org/10.1146/annurev.immunol.17.1.701; b) J. Zamorano, M.D. Rivas, M. Pérez-G, Interleukin-4: A multifunctional cytokine, Immunologia 22 (2003) 215-224
[44] C. A. Lipinski, F. Lombardo, B. W. Dominy, P. J. Feeney, Experimental and computational approaches to estimate solubility and permeability in drug discovery and development settings, Adv. Drug Deliv. Rev. 46 (2001) 3–26. https://doi.org/10.1016/S0169-409X(00)00129–0.
[45] M.D. Shultz, Two decades under the influence of the rule of five and the changing properties of approved oral drugs, J. Med. Chem. 62 (2019) 1701-1714. https://doi.org/doi: 10.1021/acs.jmedchem.8b00686.
[46] J. Chun, L. Han, M. Y. Xu, B. Wang, M. S. Cheng, Y. S. Kim, The induction of apoptosis by a newly synthesized diosgenyl saponin through the suppression of estrogen receptor–α in MCF–7 human breast cancer cells, Arch. Pharm. Res. 37 (2014) 1477–1486. https://doi.org/10.1007/s12272–013–0279–z.
[47] Y. Junchao, W. Zhen, W. Yuan, X. Liying, J. Libin, Z. Yuanhong, Z. Wei, Ch. Ruilin, Z. Lu, Antitrachea inflammatory effects of diosgenin from *Dioscoreanipponica* through interactions with glucocorticoid receptor α, J. Int. Med. Res. 45 (2017) 101–113. https://doi.org/10.1177/0300060516676724.
[48] M. Veurink, M. Koster, L.T. Berg, The history of DES, lessons to be learned, Pharm World Sci. 27 (2005) 139–143. https://doi.org/10.1007/s11096–005–3663–z
[49] A.K. Shiau, D. Barstad, P.M. Loria, L. Cheng, P.J. Kushner, D.A. Agard, G.L. Greene, The structural basis of estrogen receptor/coactivator recognition and the antagonism of this interaction by tamoxifen, Cell 95 (1998) 927-937. https://doi.org/10.1016/s0092–8674(00)81717–1.
[50] M. J. Chen, M. D. Creinin, Mifepristone with buccal misoprostol for medical abortion: a systematic review, Obstet. Gynecol. 126 (2015) 12–21. https://doi.org/10.1097/AOG.0000000000000897.
[51] B. Kauppi, C. Jakob, M. Färnegårdh, J. Yang, H. Ahola, M. Alarcon, K. Calles, O. Engström, J. Harlan, S. Muchmore, A.K. Ramqvist, S. Thorell, L. Ohman, J. Greer, J.A. Gustafsson, J. Carlstedt-Duke, M. Carlquist, The three-dimensional structures of antagonistic and agonistic forms of the glucocorticoid receptor ligand-binding domain: RU-486 induces a transconformation that leads to active antagonism, J. Biol. Chem. 278 (2003) 22748–22754. https://doi.org/10.1074/jbc.M212711200.
[52] R. D. Malmstrom, S. J. Watowich, Using free energy of binding calculations to improve the accuracy of virtual screening predictions, J. Chem. Inf. Model. 51 (2011) 1648–1655. https://doi.org/10.1021/ci200126v.
[53] A. Castro–Alvarez, A. M. Costa, J. Vilarrasa, The performance of several docking programs at reproducing protein–macrolide–like crystal structures, Molecules 22 (2017) 136. https://doi.org/10.3390/molecules22010136.